NASA Contractor Report 191578

# Calibration of HYPULSE for Hypervelocity Air Flows Corresponding to Flight Mach Numbers 13.5, 15, and 17

John Calleja and Jose Tamagno

*General Applied Science Laboratories, Inc.*
*Ronkonkoma, New York*

Contract NAS1-18450
December 1993



National Aeronautics and Space Administration

**Langley Research Center**
Hampton, Virginia 23681-0001

## ACKNOWLEDGEMENTS

This work was performed in partial fulfillment of NASA Contract NAS1-18450 Task Assignment 27, Subtask 2.2 entitled, "Facility Test Section Flow Characterization," with Mr. Griffin Anderson the NASA program manager. Part of the Mach 15 data, which is included in this report for completeness, was obtained under contract F415735 from Pratt and Whitney Aircraft Co., West Palm Beach, Florida, with Dr. W. Watkins serving as Program Manager and Mr. J. Delametter as Test Engineer. In addition to the aforementioned, the authors gratefully acknowledge the efforts of the following individuals:

| | |
|---|---|
| *Dr. John I. Erdos* | *GASL Program Manager* |
| *Mr. Richard E. Trucco* | *Flow Visualization* |
| *Mr. Robert J. Bakos* | *Technical Support* |
| *Mr. Lawrence Danziger* | *Instrumentation Support* |

SUMMARY

A series of air calibration tests were performed in GASL's HYPULSE facility in order to more accurately determine test section flow conditions for flows simulating total enthalpies in the Mach 13 to 17 range. Present calibration data supplements previous data and includes direct measurement of test section pitot and static pressure, acceleration tube wall pressure and heat transfer, and primary and secondary incident shock velocities. Useful test core diameters along with the corresponding free-stream conditions and usable testing times were determined. For the M13.5 condition, in-stream static pressure surveys showed the temporal and spacial uniformity of this quantity across the useful test core. In addition, finite fringe interferograms taken of the free-stream flow at the test section did not indicate the presence of any "strong" wave system for any of the conditions investigated.

## TABLE OF CONTENTS

## TABLE OF CONTENTS (cont'd)

## LIST OF TABLES

## LIST OF FIGURES

## LIST OF FIGURES (cont'd)

## 1.0 INTRODUCTION

The NASA/GASL Expansion Tube Facility (now called HYPULSE) was specifically developed by NASA as a means of generating hypervelocity flows with relatively low levels of molecular dissociation[1]. It was considered very well suited for conducting hypervelocity aeroheating studies, albeit with usable test times in the submillisecond range. However, practical operability appeared limited to a narrow range of test conditions. Recently, the applicability of HYPULSE for studies of hypersonic hydrogen-air mixing and combustion was demonstrated at GASL[2]. The available test times in these experiments were brief, on the order of .3 to .6 milliseconds. Despite this limitation, useful data was obtained through the use of state-of-the-art fast response instrumentation and by properly sizing models to permit the establishment of steady flow during the initial portion of the available test time. Moreover, important progress was made in the search for "alternate" test conditions which produce adequate test times (not less than .3 milliseconds) and flow quality (steadiness of core pitot pressure to within 10% over the test time).

While HYPULSE was in service at NASA/Langley, it was operated primarily at a condition which approximated atmospheric flight at Mach 17. Two other similar test conditions were also available, which used He and $CO_2$, instead of air as the test gas. The facility was then moved to GASL, where it was refurbished and upgraded as part of the NASP program. GASL then performed the first successful hydrogen-air mixing and combustion tests at NASA's Mach 17 test condition[2]. However, the desire to acquire fundamental data on mixing and combusting flows under test conditions simulating a wider range of flight Mach numbers prompted research for; 1) obtaining such test conditions, and 2) conducting an in-depth calibration to accurately quantify test section flow field properties at these conditions.

As a result, GASL was able to develop two additional operating points, one producing a total enthalpy corresponding to flight at Mach 13.5, and another with a total enthalpy corresponding to Mach 15 flight. The present work reviews existing calibration data[2,3,4] at

the Mach 17 test condition and extends it to include detailed surveys of the test core. Also, extensive test flow calibration data at the Mach 13.5 and 15 test conditions was obtained. Measured data included acceleration tube exit pitot pressure surveys on two meridional planes for various axial stations at and downstream of the tube exit plane, as well as accurate measurement of acceleration tube wall static pressure and secondary shock velocity. This data yielded a sufficient numerical data base from which nominal flow properties could be calculated and useful test cores defined. This test program also served to reemphasize the run-to-run repeatability of test conditions.

Along with the aforementioned measured quantities, an attempt was made to measure the in-stream static pressure at the test section for the Mach 13.5 condition. This was accomplished through the use of Pinckney type static pressure probes[5] placed within the free stream flow. The purpose of this exercise was twofold: 1) ascertain the state of uniformity (i.e., existence of any radial and/or axial gradients) of the static pressure across the test core, and 2) determine if a ratio other than unity exists between the measured wall and instream static pressure. Furthermore, since there was evidence that the state of the boundary layer affects the quality of the test section flow, the acceleration tube wall was instrumented with thin-film heat flux gages. These gases provided information on the state of the boundary layer (i.e., laminar, transitional, turbulent) and how it evolves as the test gas traverses the tube. Also, the fast response nature of these gages, in conjunction with acceleration tube wall pressure transducers, permitted them to be utilized as shock arrival timing devices.

Although test flow velocity at the HYPULSE Mach 17 operating point virtually duplicates that in a scramjet combustor, the static pressure (1.8 kPa / 0.25 psia) is well below that necessary to simulate a practical scramjet combustor entrance flow. Therefore, a 5.6:1 area ratio axisymmetric diffuser was attached at the end of the acceleration tube for the purpose of raising the freestream static pressure to levels which are more consistent with levels encountered within the NASP flight regime. Also, as part of this work, existing calibration data for this diffuser has been supplemented by additional instream measurement (pitot and

static pressure surveys) and flow visualization diagnostics. The results of these tests will be presented at a later date as an addendum to the present report.

During the course of these experiments, minor refinements were made to GASL's existing Laser Holographic Interferometer (LHI). The system can obtain, using the single plate/double exposure method, either finite or infinite fringe holograms. These holograms enable the researcher to detect virtually any wave system present in the flow field, as well as boundary layer profiles. Further analysis can be made based on the number of fringes as well as the fringe shifts; i.e., assessment of wave intensity and density contours (with a knowledge of the local Gladstone-Dale constant for the test gas).

## 2.0 FACILITY DESCRIPTION AND OPERATION

HYPULSE is a 6-inch diameter, 115 foot long expansion tube originally built by NASA LaRC, of which a perspective view of the present arrangement at GASL can be seen in Figure 1.

The operation of an ideal expansion tube (as proposed in Ref. 6) can be most easily described with reference to the distance-time (x-t) diagram shown in Figure 2. An expansion tube is physically similar to a shock tube with the addition of a secondary diaphragm which separates the driven tube into two sections; an intermediate tube, closest to the driver, and an acceleration tube further downstream. Initially, the driver tube (region 4 in the x-t diagram) is filled to high pressure, preferably with a low molecular weight gas such as helium or hydrogen. Although NASA frequently ran with hydrogen as the driver gas, GASL uses helium for safety reasons, despite the fact that helium requires an order of magnitude higher pressure to achieve the same performance as hydrogen. (Facility performance, as measured by the attainable total pressure and total enthalpy level, improves with increasing ratio of driver-to-intermediate tube sound speed.) The intermediate tube (region 1) is filled with the desired test gas to a pressure which is generally subatmospheric. the acceleration tube, denoted region 10, is filled with a third (acceleration) gas at an even lower pressure.

The flow is initiated by a controlled bursting of the primary diaphragms. The resulting series of compression waves rapidly coalesce into a normal shock wave which proceeds through the intermediate chamber and creates the flow in region 2. Upon striking and rupturing the secondary diaphragm, the shock (now referred to as "secondary") acquires a higher Mach number as it moves through the acceleration chamber, leading to the flow in region 20. To equilibrate the pressure and velocity from region 2 to 20, a system of unsteady upstream-facing expansion waves is generated which propagate into region 2 and accelerates the test gas to the high velocity in region 5. The test section, which receives the test gas, is located at the exit of the acceleration tube. The available testing time is the

period between the arrival of the acceleration gas/test gas interface and any waves which significantly disrupt the otherwise uniform test flow. It is important to note that the test gas is processed first by the traveling primary shock and secondly by the expansion wave system. It is not brought to rest until after it passes through the test section, unlike a conventional wind tunnel employing a converging-diverging nozzle. The problem of dissociation and recombination of the test gas at hypersonic flow conditions are thereby minimized, and the problem of driver gas contamination that may occur during shock reflection (as in a shock tunnel) is avoided.

Adjustments to the actual x-t diagram to achieve a particular operating condition for the expansion tube are made by varying driver gas sound speed and pressure, as well as intermediate and acceleration gas pressures, and by changing the relative lengths of the intermediate and acceleration tubes by placing the secondary diaphragm at different locations. This was the approach taken in order to expand the range of satisfactory flow conditions "off" the Langley nominal Mach 17 condition. The inherent disadvantage of the Mach 17 condition is the relatively low value of static pressure (~ .25 psia). This pressure level is not adequate as an inlet pressure for scramjet combustor mixing and combustion experiments, thus the design and fabrication of a contoured diffuser was undertaken (under separate contract) in an attempt to increase the free-stream static pressure by roughly an order of magnitude, yet with only a minimal loss of velocity [3,7].

The Mach 13.5 conditions were developed in an attempt to raise free stream static pressure and test time without the use of a converging section (diffuser), although at a lower velocity than that of the Mach 17 case. This eliminated some of the difficulties incurred with non-ideal diffuser performance, although the useful test core diameter is comparable to that produced with the diffuser. The Mach 15 condition was developed as a derivative of the Langley Mach 17 condition and retains similar static pressure levels to the Mach 17 case, however at somewhat lower velocity.

The M13.5 and M17 tests performed in the present test series used unheated helium as the

driver gas, while the M15 tests used a 95% He/5% $N_2$ blend (by mole fraction) as the driver gas. A nominal driver pressure of 38 MPa (5500 psi) was used for the M13.5 low pressure, M15, and M17 conditions, and 52 MPa (7500 psi) was used for the M13.5 high pressure condition. Initial driver, test, and acceleration gases were at ambient temperature prior to testing (typically 20°C/68°F) for all tests. Dry air and nitrogen was used as test and acceleration gases, respectively, with the exception of the M17 condition, which used dry air for both test and acceleration gases (see footnote[1]). The secondary diaphragm material separating the intermediate and acceleration chambers for all tests was 0.5 mil thick MYLAR™, a polyester film manufactured by DuPont. Primary diaphragms were manufactured from type 304 stainless steel and were carefully scored to maintain a ± 5% error band on run-to-run rupture pressure. A summary of facility operating parameters is given in Table 1.

---

[1] This was done in order to be consistent with the original Langley Mach 17 operating condition and previous calibration data[2,3,4]. Results obtained using $N_2$ as the acceleration gas at a slightly lower initial pressure (45.0 $\mu$mHg opposed to 54.0 $\mu$mHg used in these tests) will be presented at a later date in an addendum discussing the calibration of the diffuser.

## 3.0 CALIBRATION OF TEST FLOW

### 3.1 Instrumentation

The instrumentation used in these current set of calibration tests permitted direct measurement of acceleration tube wall static pressure and heat-flux, primary and secondary shock velocities, acceleration tube exit plane pitot pressure and in-stream static pressure. All subsequent flow properties were calculated based on this data. In addition, flow visualization in the form of finite-fringe interferograms was used as a means to identify flow structures associated with measured pressure gradients.

Tube wall static pressure measurements were obtained using PCB™ piezoelectric type pressure transducers mounted either slightly recessed from (intermediate chamber) or flush to (acceleration chamber) the respective tube wall. A special high-sensitivity transducer was used 1.0" upstream of the acceleration tube exit to insure accurate measurement of wall static pressure in the 0-5 psia range.

Heat transfer rates to the acceleration chamber wall were obtained using GASL developed thin-film heat transfer gages[8]. These gages were mounted flush to the chamber wall and provided information on the instantaneous surface temperature of each respective thermoresistor. These temperature histories were then reduced numerically to obtain heat transfer rates, which in turn served to indicate the state of the boundary layer aft of the secondary shock. Knowledge of the state of the boundary layer here is important in that there is some experimental evidence which would indicate that the quality of the test flow is strongly influenced by the occurrence of transition of the tube wall boundary layer during the test period.

Primary (intermediate chamber) and secondary (acceleration chamber) shock velocities were determined from shock arrival times at various transducer port locations. Both pressure transducers and heat-flux gages exhibit response times on the order of 1 microsecond and

were therefore dually utilized as shock timing devices. Schematic diagrams are shown in Figure 3 for the two configurations of intermediate to acceleration chamber length ratios used in this series of tests. Specifically, for the M13.5 conditions the secondary diaphragm was placed in the downstream position, and for the M15 and M17 conditions it was placed in the upstream position. Primary and secondary incident shock velocities were calculated as mean values between respective instrumentation port locations, shown on the diagrams. Secondary shock velocity data from all tests at a particular condition were curve fit and extrapolated to the acceleration chamber exit (test section) to obtain $U_{s,2}$.

A five-probe survey rake was used at the test section to measure flow pitot pressure across the acceleration tube exit plane. This rake is shown installed in the test section in Figure 4. The same type of PCB™ pressure transducers as those used in the intermediate and acceleration chamber walls were used in the rake probes. Probe tip design was chosen to protect the transducers from direct particle impingement and possible damage and the interior volume of the probes was minimized to retain high-frequency response. Probes were placed on 1.0 inch centers for a rake span covering a 4.0 inch diameter. Also, the rake was able to accept Pinckney[6] type static probe tips for measurement of in-stream static pressure.

Several tests were made with the pitot rake stationed at various axial locations downstream of the acceleration tube exit plane. Through a combination of axially relocating the model/rake support in 2.0 inch increments and repositioning the acceleration tube with respect to the test section, it was possible to locate the rake from the exit plane (x=0.0) to a point 8.0 inches downstream of the exit plane (x=8.0). In order to increase the spacial resolution of the flowfield measured pitot pressure, tests were made with the rake at the centerline (y=0.0) and raised 0.5 inch above the centerline (y=0.5).

In-stream static pressure was measured for the M13.5 low pressure condition in order to verify the radial uniformity of static pressure within the test flow. This was accomplished by fitting two of the probes on the rake with static pressure tips (Figure 5) following the

design of Pinckney[6]. Both PCB™ and Kulite™ pressure transducers were used in conjunction with these tips. In-stream static pressure surveys could not be obtained for the M15 and M17 conditions due to the relatively low static pressures encountered. (The major advantage of the Kulite gages is their relatively small size, allowing small probe design for adequate resolution of the in-stream static profile. However, their output sensitivity (mV/psi) is so low that they cannot be used with confidence to measure the low static pressures associated with these conditions.)

### 3.2 Data Acquisition and Reduction

Facility and test flow data was acquired and stored using LeCroy™ model 6810 4-channel transient waveform digitizers with sufficient on-board memory to store 512K samples per channel. Each data channel was sampled at a rate of 500 kHz with 12-bit vertical resolution. Power for the digitizers was supplied by two LeCroy™ model 8025 high-power CAMAC crates. The entire data acquisition system (DAS) was controlled with an IBM compatible PC (a COMPAQ™ 386/20) and vendor supplied software ("Waveform CATALYST version 2.6").

The power supply control units for the PCB™ pressure transducers were supplied by PCB™, while the Kulite™ gages were powered by a GASL supplied constant DC source. The heat-flux gages were powered by a low-noise linear DC power supply and controlled by a GASL manufactured control unit.

All of the raw pressure and heat transfer data was reduced through the PC-based program XT. (This software was previously developed at GASL.)

### 3.3 Data Uncertainty

While the total uncertainty in the measured pressure data may stem from several sources, by far the most dominant source arises from the uncertainty in the calibrated sensitivities of the pressure transducers for the range of interest encountered in these tests. Therefore, PCB™ type (piezoelectric) pressure transducers that were deemed important for pressure measurements underwent a sensitivity assurance evaluation both prior to and following the test series. Based on these calibrations, manufacturer's specifications, and systematic errors which are inherent in the measurement, the uncertainty in pressure measurements using these gages is estimated to be within ± 3%. Uncertainty for the Kulite™ gages has not been estimated, although it is believed to be higher than that of the PCB™ gages.

Post-test series calibrations were not performed for the heat transfer gages since their purpose was mainly to yield shock timing data and qualitative information regarding the state of the boundary layer. However, based on previous[8] as well as present work, the uncertainty in heat transfer measurements is estimated to be within ± 5%.

## 4.0 FLOW VISUALIZATION

The HYPULSE non-intrusive flow diagnostics system includes a ruby-laser based holographic interferometer which was used in the present tests to image the flowfield at the test section. Improvements were made to the pre-existing LHI system by the addition of a laser intercavity pinhole and minor adjustments to the system layout. Figure 6 shows a diagram of the system as it existed during these tests.

## 5.0 CALCULATION OF FREE-STREAM CONDITIONS

Freestream conditions were calculated using GASL's in-house developed program EQSTATE. This code accepts inputs of the upstream conditions (pressure, temperature, and velocity), undissociated species mass fractions, flow deflection angle, and flags for equilibrium or frozen chemistry upstream and downstream of the shock. An equilibrium chemistry calculation is then carried out utilizing the CREK chemistry package developed by Pratt[9] to yield freestream and post-shock static and stagnation properties, as well as the gas composition of each state in terms of mass and mole fractions.

The freestream velocity ($U_5$) was computed using a PC-based code developed at GASL and is based on Mirels' theory [10, 11], which accounts for boundary layer growth. Measured primary and secondary shock Mach numbers, quiescent intermediate and acceleration gas pressure, and intermediate and acceleration chamber lengths are used as inputs to the code.

In cases where the arrival times of both the secondary incident shock and the contact surface (test/acceleration gas interface) could be accurately measured at the test section, the freestream velocity $U_5$ was also computed using the simple relation

$$\frac{1}{U_5} = \frac{\Delta t}{l_{acc}} + \frac{1}{U_{s,2}} \qquad (1)$$

where $\Delta t$ is the time between the arrival of the secondary shock and the interface at the test section, $l_{acc}$ is the acceleration chamber length, and $U_{s,2}$ is the secondary shock velocity at the end of the acceleration chamber. This method was employed as verification of the calculation made using the analysis of Mirels' for the Mach 13.5 conditions. The two methods showed excellent agreement, with the comparison shown in Table 3. Freestream velocities that were calculated using the above equation are mean values over all runs at that condition. Centerline and just-off-centerline (± .5") pitot pressure time histories were

used to obtain $\Delta t$ (Figures 10 and 16). Verification of the freestream velocity could not be made at the Mach 15 and 17 conditions since the proximity of the interface to the secondary shock does not allow accurate measurement of $\Delta t$ in these cases.

Since freestream static temperature ($T_5$) was not measured directly in these tests, it was necessary to assume a temperature to be used as input to EQSTATE along with mean values of static pressure ($P_5$) and velocity ($U_5$) for each condition. This "guessed" temperature was varied and the process repeated until the calculated value of the post-normal shock stagnation pressure matched the measured mean value of test core pitot pressure ($P_{t,2}$). Measured mean values are listed in Table 2 and calculated flow properties are listed in Table 3.

## 6.0 DISCUSSION OF RESULTS

This section presents results obtained and briefly discusses each of the five cases investigated: four of them using air and one using oxygen as the test gas The use of 100% oxygen as a test gas was suggested in Ref. 12 as means to compensate for kinetic rate limitations arising from low pressure combustion processes. In all cases, pitot to static pressure ratio profiles are presented. The values of static pressure used in these plots can be found in Table 2 and represent mean values for data taken at the wall of the acceleration chamber at the exit. Mean core pitot pressure values for each condition are also given in Table 2 for $0 \leq x \leq 2.0$ inches, where x denotes the axial distance downstream of the acceleration tube exit plane. Computed flow properties based on measured values can be found in Table 3.

Usable testing time for all conditions was determined primarily from the pitot pressure traces within the test core as well as the acceleration tube wall pressure and heat-flux histories near the exit. The "test-time" for a particular condition is defined as "the period of steady flow between the arrival of the test gas and any waves which disrupt this flow at the test section." Thus, the period of time where core pitot pressure, wall static pressure and wall heat flux remained relatively constant prescribed the test time in each case. All figures in this section that present these quantities have been time averaged ("smoothed") over 10 $\mu$sec.

### 6.1 M13.5 "Low Pressure" (LP) Test Condition

#### 6.1.1 Air Test Gas

This condition was developed to simulate combustor entrance conditions consistent with the NASP flight at Mach 13.5. Since it possesses a sufficiently high static pressure level (18 kPa/2.6 psia), mixing and combustion tests can be performed without the use of a

converging section.

Figure 7 shows a composite pitot-to static pressure ratio profile for this condition with the rake at various axial locations with respect to the acceleration tube exit plane. (The combustor model inlet is typically positioned at x = 1.0 inches. + denotes downstream of the acceleration tube exit plane.) The plot shows that axial gradients in pitot pressure are not apparent for $0 \leq x \leq 4.0$ inches. However, at x = 8.0 inches there is a discernable decrease in the overall magnitude of the profile and a reduction in core diameter due to acceleration tube exit expansion effects. Figure 8 shows the individual pitot to static pressure profiles at each axial location. Figure 8(b) displays the profile at x = 2.0 inches. For this case, pitot data was obtained with the rake positioned horizontally as well as vertically. It can be seen that the data obtained in both cases agree quite well, thus demonstrating the radial symmetry of the flow field.

Figure 9 presents in-stream static pressure data taken across the half-plane at x = 2.25 inches. The data has been normalized to the average measured wall static pressure taken at the acceleration tube exit. It is evident from this data that no significant radial static pressure gradients could be measured in the test flow. This would infer that two-dimensional perturbations which would otherwise degrade the uniformity of test flow static pressure are either absent or are weak enough such that their influence is, for all practical purposes, insignificant.

A two-inch diameter test core is defined for this test condition, which possesses a 7.5% standard deviation for the mean value of $P_{t,2}/P_5$. It has been estimated that the reason for the relatively narrow core and associated pitot pressure field is primarily due to a thick turbulent boundary layer within the test gas portion of the flow (region 5). In the acceleration gas (region 20), the free-stream Reynolds number is on the order of $6.0 \times 10^5$ $m^{-1}$. In traversing the test/acceleration gas interface (region 20 to region 5), the freestream Reynolds number increases to $1.5 \times 10^6$ $m^{-1}$.

Figure 10 shows typical pitot pressure traces for this condition with the rake positioned on the centerline 2.0 inches downstream of the acceleration tube exit plane. Figure 11 shows typical wall static pressure and temperature histories, as well as wall heat flux. Note that the pitot traces clearly indicate that the test gas interface arrives about 160 $\mu$sec after shock arrival. In this case, the test time is considered to be the 600 $\mu$sec following the arrival of the interface. It is quite evident from the wall temperature history that the boundary layer is laminar in the acceleration gas portion of the flow sequence, and transitions to a turbulent state immediately following the test/acceleration gas interface. Also note the relatively large random fluctuations in region 5 compared to region 20 for the pitot pressure histories on and close to the centerline (i.e.: within the test core).

A wave analysis showed that the unsteady secondary expansion waves reflected from the driver/test gas interface should arrive at the test section almost simultaneously with the test gas. This system of waves could manifest itself as fluctuations in pitot pressure. In fact, at the M17 test condition, it will be shown that the arrival of the reflected expansion coincides with the appearance of rather large random disturbances in an otherwise "quiet" flow.

Examination of the static pressure history reveals a slight linear variation of this quantity over the 600 $\mu$sec testing time (Figure 11). This effect can be partially accounted for by either an extended secondary expansion from region 2 to 5 (refer to Figure 2) necessary to match the velocity of the test/acceleration gas interface, which is continually accelerated through viscous effects[10, 11], or by the simultaneous arrival at the test section of the reflected expansion wave system with the test gas. On the other hand, the pitot pressure does not increase at the same rate as the static pressure during the test time, which results in a slight temporal decrease in $M_\infty$, as shown in Figure 12.

In order to minimize the effect of such an increase in static pressure, values for $P_5$ were obtained by performing a time average over a pre-defined window of shorter duration (400 $\mu$sec.) than the full available test time, which is suitable for combustion testing. This resulted in a 25% variation in static pressure from the mean value (18.2 kPa) averaged over

all tests. Similarly, this method was employed in the reduction of pitot pressure histories to maintain consistency and resulted in a mean value of 386 kPa over the 2.0 inch diameter test core.

### 6.1.2 Oxygen Test Gas

In its current configuration, the HYPULSE expansion tube may be pressure limited for conducting certain types of combustion experiments. That is, the (air) test gas static pressure may be low enough to cause chemical kinetic rate limitations on the hydrogen-air ignition and combustion processes. To circumvent this limitation, the use of a pure oxygen test medium was proposed as a means to increase the partial pressure, and hence collision frequency, of oxygen. This has been found to be an effective means of promoting complete combustion within the available length of the combustor model (0.7 - 1.0 m). As a result, calibration tests were performed at the Mach 13.5 LP condition in order to accurately define combustor inlet flow properties for a pure oxygen test gas.

A HYPULSE operating point was selected for oxygen so as to produce test conditions closely resembling those of air at Mach 13.5. Figure 13 displays calibration results in terms of the pitot-to-static pressure ratio at x=2.0 inches downstream of the acceleration tube exit plane. As can be seen, the resulting profile exhibits a close similarity with that obtained for air.

Measured mean flow properties and test flow conditions calculated from measured data are presented in Tables 2 and 3, respectively. The resemblance of flow properties between the air and oxygen test gases for this condition allows the direct comparison of combustor performance achieved with each respective gas.

A finite fringe interferogram was taken for the pure oxygen test gas case with the rake positioned horizontally 2.0 inches from the tube exit, as shown in Figure 14. Fringe

displacements can clearly be seen for the probe tip and wedge bow shocks.

### 6.2 M13.5 "High Pressure" (HP) Test Condition

This condition was designed to maintain the same total enthalpy and Mach number while increasing the static pressure over the M13.5 LP condition. This was accomplished by a simple scaling of all the initial gas pressures ($P_1$, $P_4$, $P_{10}$) by 1.36. The resulting increase in $P_5$ directly corresponds to this scaling and is shown, along with other measured flow data, in Table 2. Computed freestream conditions are given in Table 3. As can be seen from this table, the total enthalpy and Mach number closely matches the "low pressure" values and only the total pressure, static pressure and unit Reynold's number are significantly increased.

The purpose of calibrating HYPULSE at this operating point was twofold: 1) to demonstrate that scaling initial facility pressures carries directly over to a corresponding scaling of test flow static pressure, provided that the change in Reynolds number across the interface is such that the state of the tube wall boundary layer associated with the test flow remains unchanged, and; 2) to develop an additional condition for this enthalpy simulation that is an acceptable option for combustor inlet parametric testing. These objectives were met.

The measured test section pitot pressure profiles at x = 1.0 and 1.5 inches downstream of the acceleration tube exit plane virtually mock the low pressure case in both profile and magnitude, as expected, and are shown compositely in Figure 15. Although the average pitot-to-static pressure should be equivalent to the low-pressure case, the value is in fact slightly higher (3.7%) with a corresponding increase in free-stream Mach number (1.9%). Averaging of the wall static pressure data resulted in a mean value of 23.5 kPa, while mean pitot pressure over the 2.0-inch diameter core was 510 kPa. In-stream static pressure measurements were not made for this condition. Representative time histories of typical centerline pitot pressure, wall static pressure, wall temperature and heat flux are shown for this condition in Figure 16. Useful test time remained the same as the low-pressure case.

A finite fringe interferogram of the pitot rake positioned vertically is shown in Figure 17. Careful examination reveals small bow shock structures about the individual probe tips in the form of fringe displacements.

### 6.3 M15 Test Condition

The Mach 15 test condition was developed as an intermediate flight condition in order to bridge the gap between the M13.5 and M17 conditions. The calibration tests performed at this condition were successful in further demonstrating the ability to operate HYPULSE over a wider range of conditions.

Present calibration data, coupled with previously obtained data[13], suggest that satisfactory performance is obtained when the tube wall boundary layer remains fully laminar during the test period. The Mach 15 condition is similar to the Mach 17 condition in that the boundary layer remains laminar throughout the test flow. Driver, intermediate and acceleration gas initial pressures were identical to the Mach 17 case (Table 1), as were the intermediate and acceleration chamber gases. However, in order to tailor the test gas such that a velocity of approximately 15000 ft/s and a freestream Reynolds number low enough to maintain a laminar boundary layer within the test flow is achieved, a five percent concentration (by mole fraction) of nitrogen was introduced into the helium driver gas.

Figure 18 shows the pitot-to-static pressure profile for this condition at x=1.0 inch. Measured pitot pressure was normalized to the mean value of the wall static pressure for all runs at this condition. (In-stream static pressure measurements could not be made for this condition.) Although the profile appears to "dip" slightly about the centerline, one must bear in mind that only a limited number of runs were made at this condition. Therefore, postulation as to why this may be occurring would be purely speculative at this time. Note, however, the general repeatability of the data (as in the previous cases).

Measured data and calculated flow properties are listed in Tables 2 and 3, respectively. Typical pitot pressure traces are shown in Figure 19 and typical static pressure and wall temperature traces along with corresponding heat-transfer rates are shown in Figure 20.

A major difference between the M13.5 conditions and the M15 and M17 conditions is the

distance between the secondary shock and the test/acceleration gas interface. In the M13.5 case, the duration of the acceleration gas portion of the flow at the test section is approximately 160 $\mu$sec, as clearly shown by the pitot pressure time histories (Figures 10 and 16) and is rather well predicted by Mirels' theory [10, 11]. In the M15 and M17 cases, however, the test/acceleration gas interface is extremely close to the secondary shock. (In fact, the interface is virtually imperceptible on the pitot pressure histories in Figures 19 and 23.) This results in the test gas velocity being virtually equal to the secondary shock velocity and again is fairly well predicted by Mirels' theory [11]. Here, the tube wall boundary layer remains laminar for the duration of the 350 $\mu$sec test period and well into the post-test flow, as indicated by the wall heat flux history in Figure 20. This is considered a very important distinction relative to the M13.5 operating points with regard to both the character of the test gas flow and the ability to find other test conditions between the M15 and M13.5 operating points.

### 6.4 M17 Test Condition

This condition was calibrated as a modified case of the Langley Nominal M17 Condition. The main difference between this condition and the Langley condition is that the quiescent acceleration gas pressure is 54.0 $\mu$mHg instead of 45.0 $\mu$mHg. The rationale for this modification emerged from a previous calibration effort [2], in which the objective to minimize pitot pressure ramping over the test time while maintaining test duration and flow velocity was successfully met.

A composite pitot-to-static pressure profile for this condition with the pitot rake positioned at various axial locations downstream of the acceleration tube exit is shown in Figure 21. A virtually inviscid 3-inch diameter core is apparent from this plot for as much as four inches downstream of the acceleration tube exit. Figure 22 shows the individual pitot-to-static pressure profiles for x = 1.0, 2.0, and 4.0 inches. As in the M15 case, the static pressure was too low to obtain valid in-stream measurements of this property using the Pinckney-type

probe.

Typical pitot pressure traces are shown in Figure 23 for this condition. Note the approximate 30 $\mu$sec duration of the acceleration gas portion of the flow indicating the proximity of the interface to the secondary shock. These traces were again used in conjunction with the wall static pressure and temperature traces (Figure 24) to determine the 300 $\mu$sec test time.

Examination of acceleration tube wall heat-transfer rate near the exit and freestream pitot pressure at the exit (Figure 24) indicate that boundary layer transition does not occur until approximately 200 $\mu$sec. into the post-test flow. By this point in the flow sequence, the static pressure has significantly increased, the flow velocity has diminished, and the previously "quiet" freestream has acquired a high degree of turbulence. However, this turbulence, which is manifested in the form of relatively large fluctuations in the static and pitot pressure, was present prior to the tube wall boundary layer transition occurrence. This suggests that larger disturbances within the test gas may be induced through other mechanisms, e.g., reflected waves off the highly turbulent interface, and not solely by boundary layer behavior.

The extended pitot trace outside of the core region (y=-2.0 in.) in Figure 23(b) shows the combined effects of both the boundary layer and the reflected expansion wave system. Boundary layer impingement is believed to be responsible for the decay of the pitot pressure, while the large random disturbances are most likely induced by the reflected expansion wave system.

## 7.0 CONCLUDING REMARKS

The completion of the calibration portion of Task 27 was carried out in GASL's HYPULSE for hypervelocity air flows in the 3800 to 5200 m/s velocity range (Mach 13.5 to 17 test conditions, respectively). Present data coupled with previous data served to accurately determine flow properties at the test section as well as define usable test times and core diameters for each condition. Additionally, these tests functioned to reemphasize the repeatability of flow conditions seldom found in high enthalpy pulse facilities.

In-stream static pressure was measured across the acceleration tube exit plane for the M13.5 "low-pressure" test condition. For this condition, the measured data did not give indication of any radial static pressure gradients within the confines of the test flow. At the Mach 15 and Mach 17 test conditions, however, the static pressure was low enough such that accurate measurements of this quantity could not be obtained given the nature of the short duration flow and the available static pressure probe/gage configuration. Therefore, flow visualization, in the form of finite fringe interferograms, provided evidence that no measurable pressure gradients exist within the test core for these conditions.

Although the in-stream measurements indicate a uniform static pressure field for the Mach 13.5 test condition, the free stream static pressure was found to differ from the wall value (as measured by a flush-mounted transducer) by as much as 20%. At present, there is no viable explanation for this discrepancy. However, it is possible that the Pinckney type probe is not sufficiently calibrated for in-stream static pressure measurements in the hypervelocity flows produced by HYPULSE.

## 8.0 REFERENCES


1. Tamagno, J., Bakos, R.J., Pulsonetti, M., and Erdos, J., *"Hypervelocity Real-Gas Capabilities of GASL's Expansion Tube (HYPULSE) Facility,"* AIAA Paper No. 90-1390, June 1990.

2. Bakos, R.J., Tamagno, J., Posillico, T., and Erdos, J., *"HYPULSE Facility Preparation, Calibration, and Initial Mach 17 Mixing and Combustion Experiments,"* GASL TR 318, October 1990.

3. Calleja, J., Tamagno, J., and Erdos, J., *"Calibration of the GASL 6-Inch Expansion Tube (HYPULSE) for Air, Helium, and Carbon Dioxide Test Gases,"* GASL TR 325, September 1990.

4. Tamagno, J., Bakos, R.J., and Pulsonetti, M.V., *"Results of Preliminary Calibration Tests in the GASL HYPULSE Facility-Expansion Tube,"* GASL TR 308, May 1989, also NASP-CR-1071, November 1989.

5. Pinckney, S.Z., *"A Short Static Pressure Probe Design for Supersonic Flow,"* NASA TN-D-7978, July 1975.

6. Trimpi, R.L., *"A Preliminary Theoretical Study of the Expansion Tube, A New Device for Producing High Enthalpy, Short Duration Hypersonic Gas Flow,"* NASA TR-R-133, 1962.

7. Bakos, R., Trucco, R., Tamagno, J., and Erdos, J., *"Experimental Determination of Scramjet Combustor Performance Parameters at Mach 13.5 and 17 Flight Conditions,"* GASL TR 327, January 1991.

8. Calleja, J., and Danziger, L., *"Performance of GASL Thin-Film Heat Transfer Gages in Tests Using a 3-Inch Diameter Valve-Actuated Shock Tube,"* GASL TM 236, January 1990.

9. Pratt, D.T., *"Calculation of Chemically Reacting Flows with Complex Chemistry,"* in Studies in Convection, Vol. II, B.F. Launder, ed. Academic Press, N.Y. 1976.

10. Mirels, Harold, *"Shock Tube Test Time Limitation Due to Turbulent Wall Boundary Layer,"* AIAA Journal, Vol. 2, No. 1, January 1964.

## 8.0 REFERENCES (Continued)


11. Mirels, Harold, *"Test Time in Low Pressure Shock Tubes,"* Physics of Fluids, Volume 6, No. 9, September 1963.

12. Bakos, R., et. al., *"Mixing, Ignition, and Combustion Studies Using Discrete Orifice Injection at Hypervelocity Flight Conditions,"* AIAA/ASME/SAE 27th Joint Propulsion Conference, Sacramento, CA , June 24-27, 1991, Paper No. AIAA-91-2396.

13. Tamagno, J., Trucco, R., Bakos, R., *"Scramjet Combustor Tests with Instream Injection at Mach 13.5 and GASL HYPULSE Facility Calibration at Mach 15,"* GASL TR 334, August 1991.

| SIMULATED CONDITION | GAS D-T-A | $P_4$(MPa) | $P_1$(mmHg) | $P_{10}$($\mu$mHg) | $L_t/L_a$ (m) | SECONDARY DIAPHRAGM |
|---|---|---|---|---|---|---|
| M13.5 HP | He-Air-$N_2$ | 52 | 17.7 | 820 | 12.12/10.02 | Mylar/0.5mil |
| M13.5 LP | He-Air-$N_2$ | 38 | 13.0 | 600 | 12.12/10.02 | Mylar/0.5mil |
| M13.5 LP | He-$O_2$-$N_2$ | 38 | 13.0 | 600 | 12.12/10.02 | Mylar/0.5mil |
| M15 | 95He/5$N_2$-Air-$N_2$ | 38 | 26.0 | 45.0 | 7.52/14.62 | Mylar/0.5mil |
| M17 | He-Air-Air | 38 | 25.7 | 54.0 | 7.52/14.62 | Mylar/0.5mil |

D-Driver, T-Test, A-Acceleration



Table 1. Facility Operating Parameters

| TEST CONDITION | STATIC PRESSURE (Pa) | CORE PITOT PRESSURE (kPa) | SECONDARY SHOCK VELOCITY (m/s) | USEFUL TEST TIME ($\mu$sec) |
|---|---|---|---|---|
| M13.5 HP | 23440 ± 965 | 510.1 ± 46.9 | 4176 ± 30 | 400 |
| M13.5 LP (Air) | 17990 ± 275 | 386.0 ± 31.7 | 4169 ± 24 | 400 |
| M13.5 LP ($O_2$) | 18400 ± 100 | 440.0 ± 22.5 | 4111 ± 17 | 400 |
| M15 | 1520 ± 70 | 105.5 ± 5.5 | 4707 ± 19 | 350 |
| M17 | 2000 ± 70 | 155.8 ± 9.0 | 5176 ± 42 | 300 |

Note: Quoted quantities represent mean values obtained from both present and previous data. Error bands represent one standard deviation $\sigma$.



Table 2. Measured Quantities

| TEST CONDITION | TOTAL ENTHALPY (MJ/kg) | TOTAL PRESSURE (MPa) | TOTAL TEMP. (°K) | STATIC TEMP. (°K) | VELOCITY (m/s) | MACH NUMBER | UNIT $Re_L$ ($x10^6$ $m^{-1}$) | $\gamma$ |
|---|---|---|---|---|---|---|---|---|
| M13.5 HP | 9.83 | 14.66 | 5840 | 2280 | 3858 (3872) | 4.19 | 1.96 | 1.294 |
| M13.5 LP (Air) | 9.88 | 10.27 | 5780 | 2350 | 3848 (3868) | 4.10 | 1.43 | 1.293 |
| M13.5 LP ($O_2$) | 9.60 | 24.28 | 5074 | 2345 | 3832 (3881) | 4.35 | 1.36 | 1.274 |
| M15 | 11.53 | 59.75 | 6865 | 1050 | 4631 | 7.31 | 0.54 | 1.333 |
| M17 | 14.04 | 152.9 | 8070 | 1140 | 5124 | 7.77 | 0.68 | 1.328 |

Note: ( ) items were computed using equation (1).



Table 3. Calculated Free-Stream Conditions

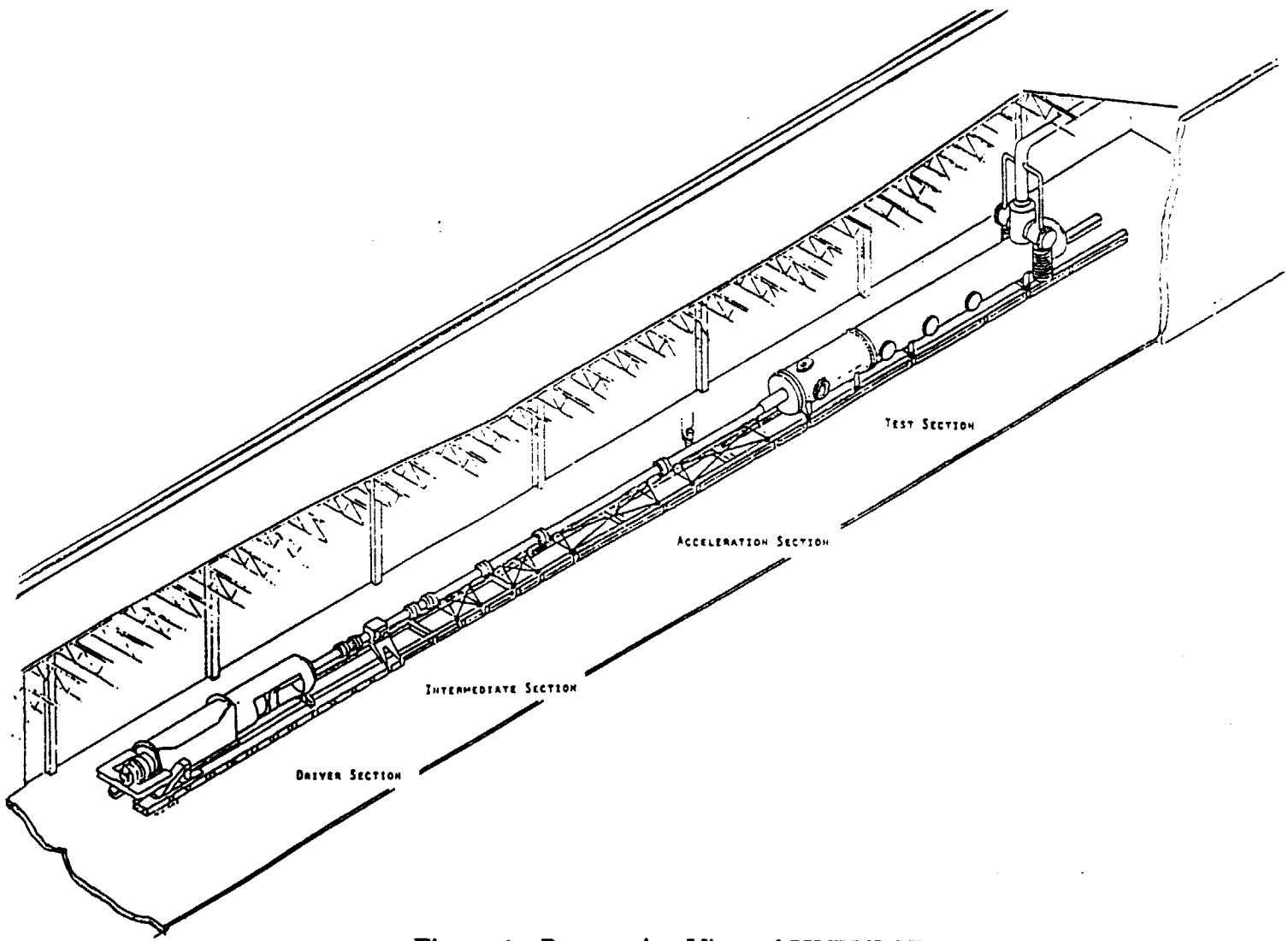


Figure 1. Perspective View of HYPULSE

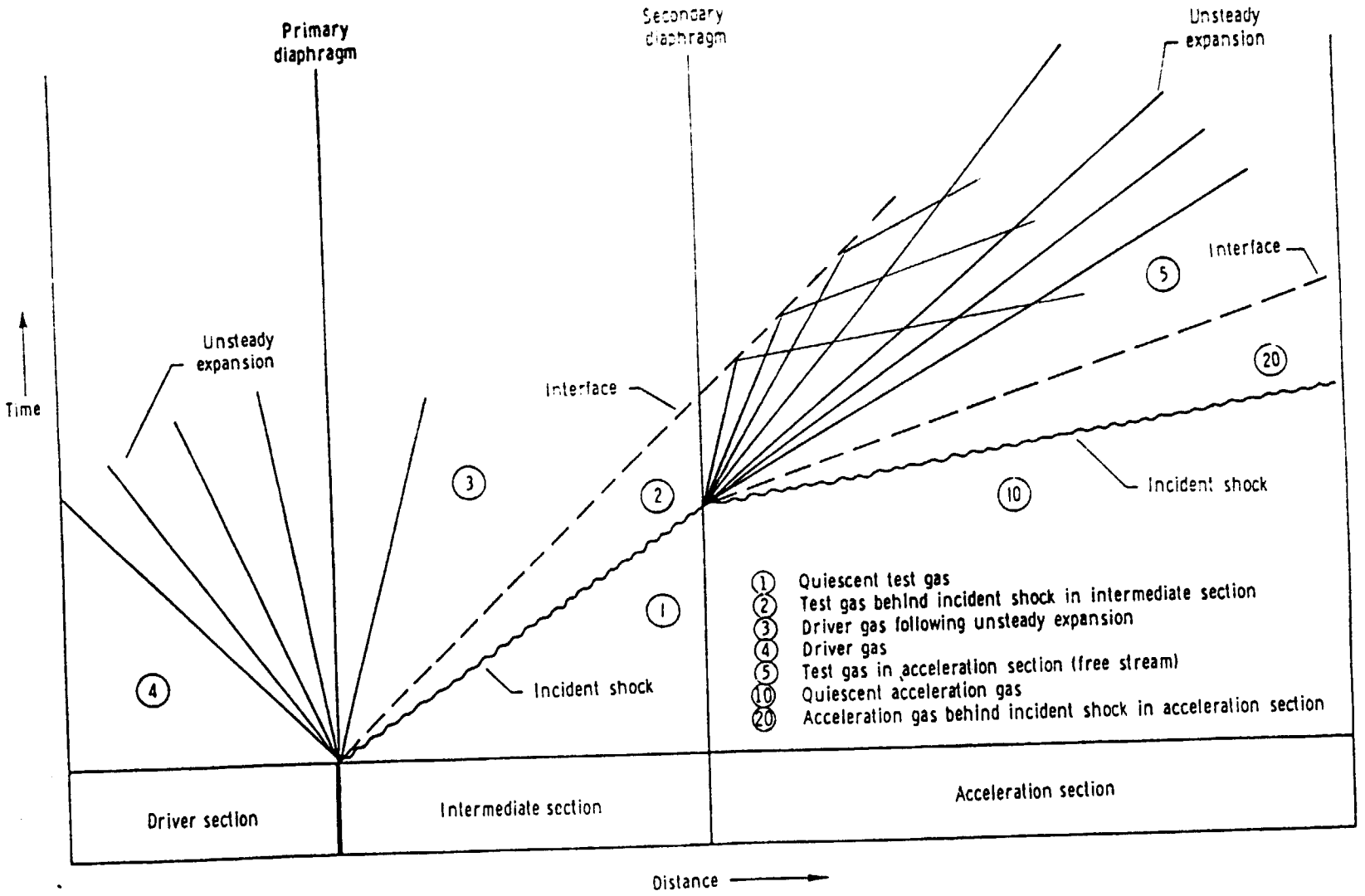


Figure 2. Distance-Time Diagram for Expansion Tube

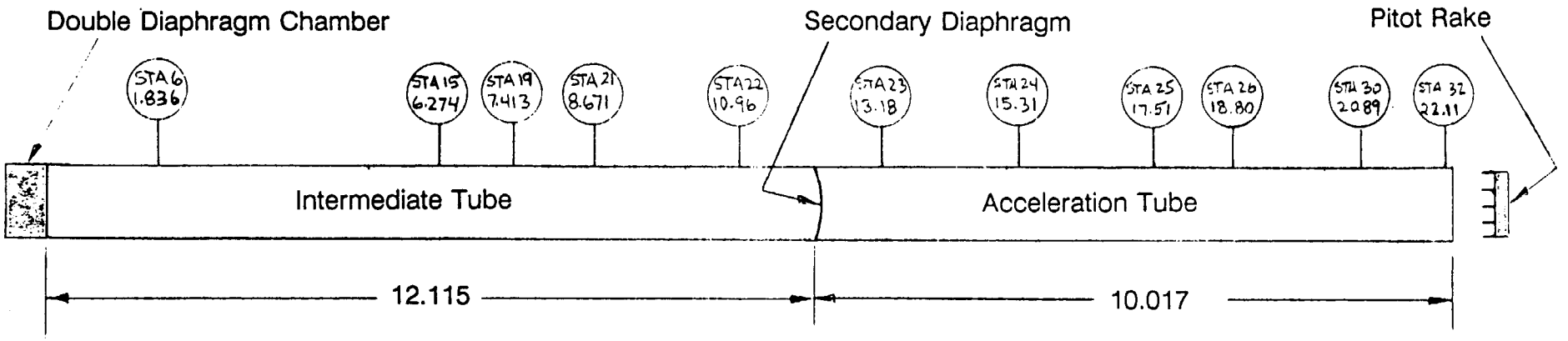


a) M13.5 Conditions

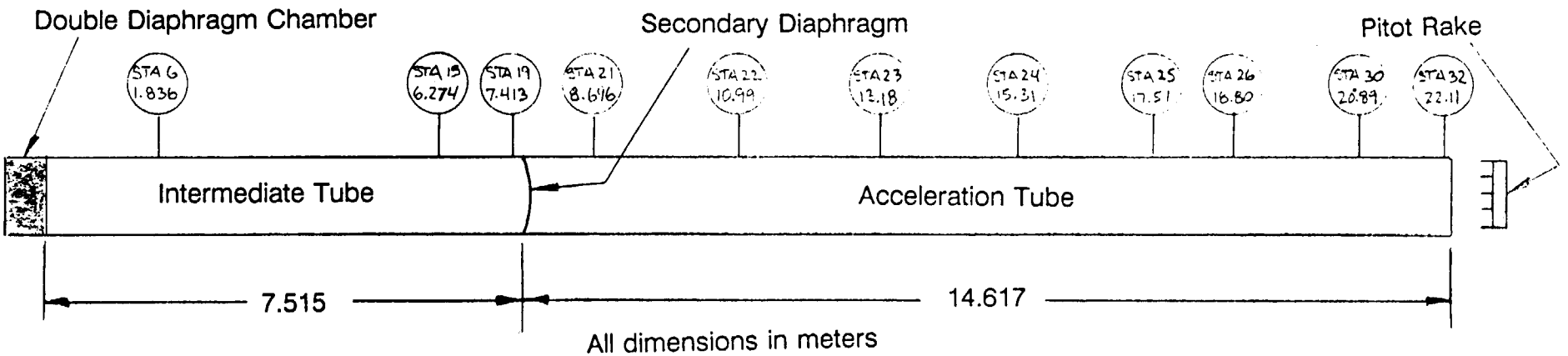


b) M15 and M17 Conditions

Figure 3. Instrumentation/Diaphragm Layout

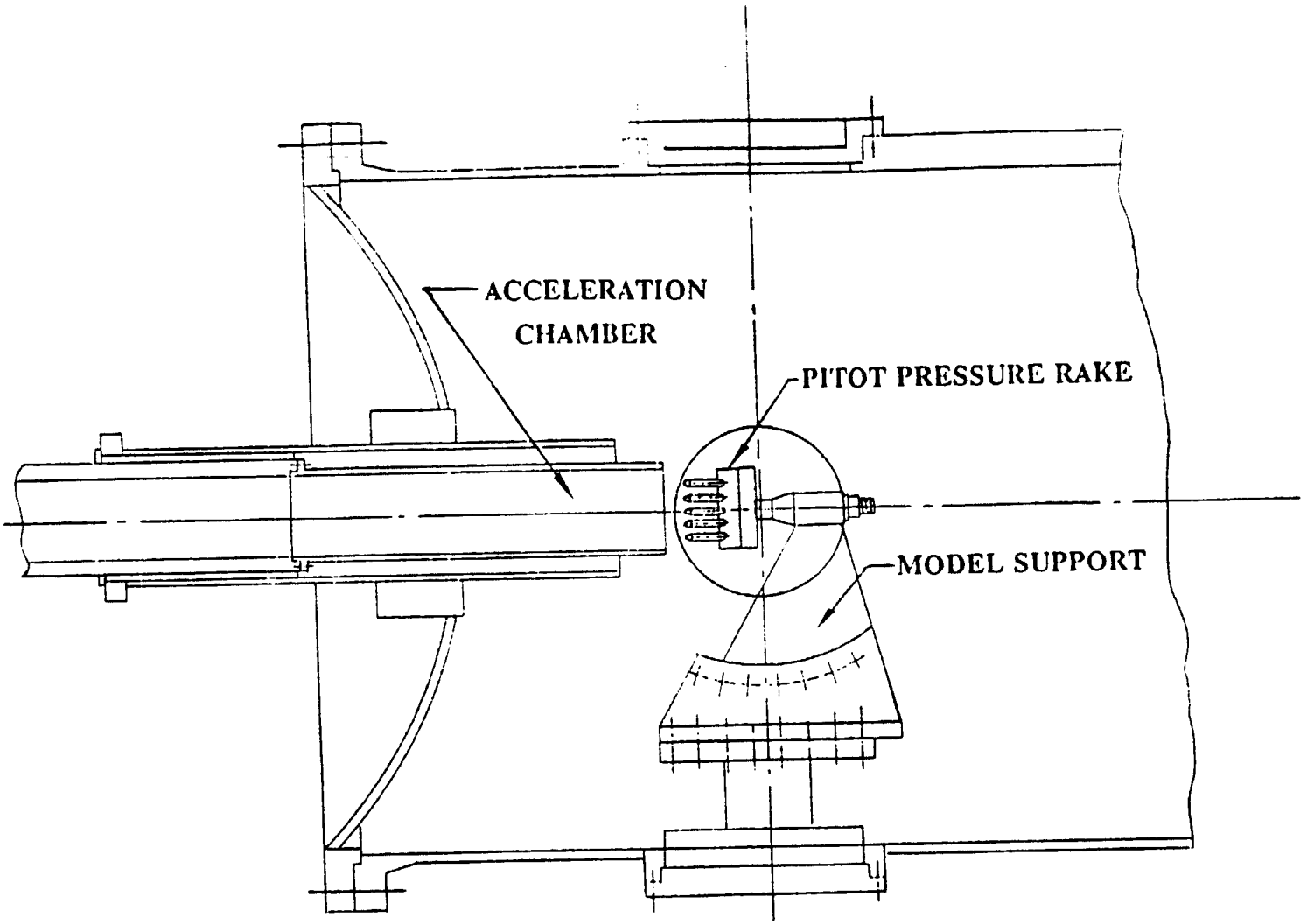


Figure 4. Pitot Pressure Rake in Test Section

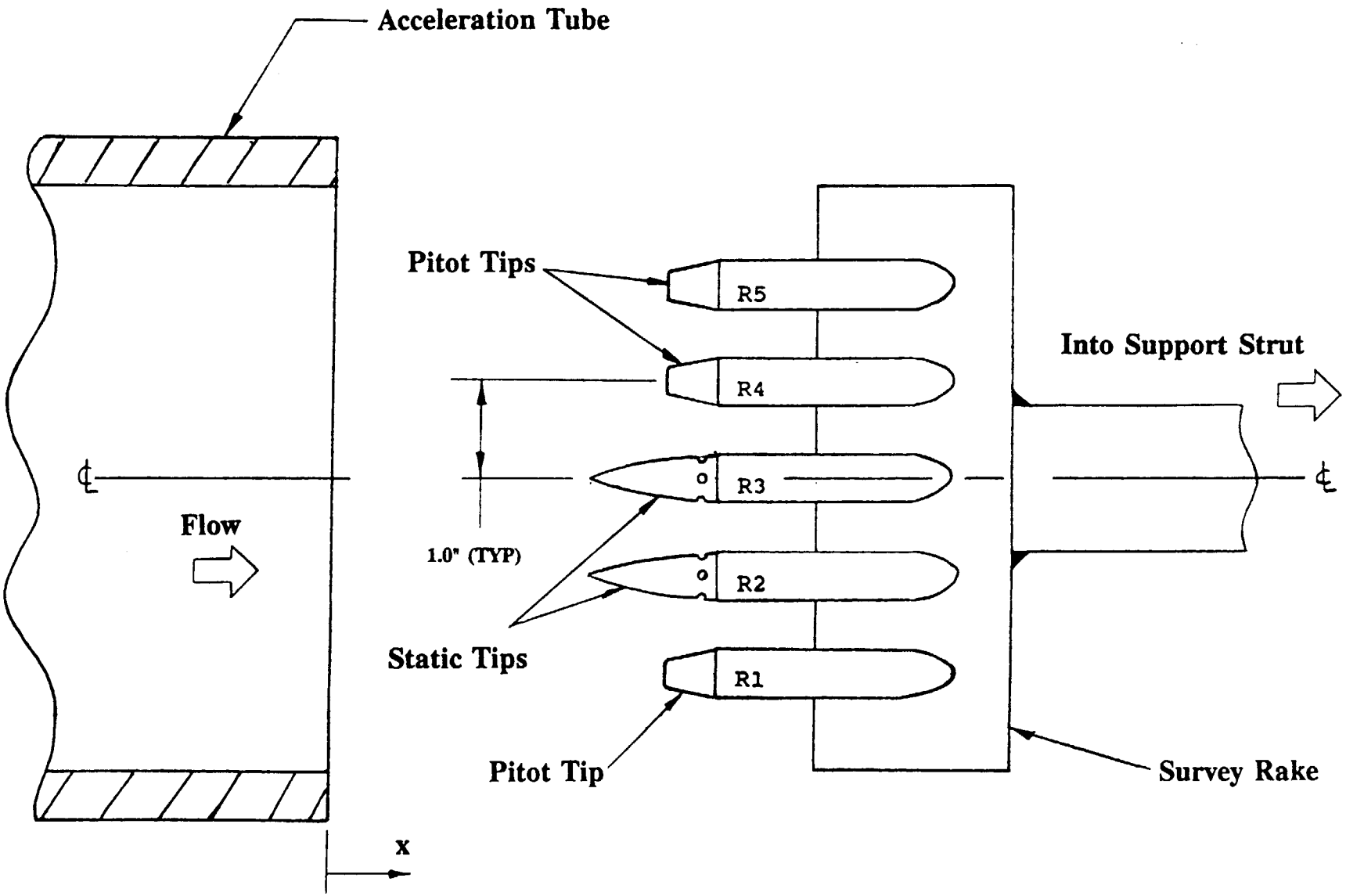


Figure 5. Rake Fitted with Static Pressure Tips

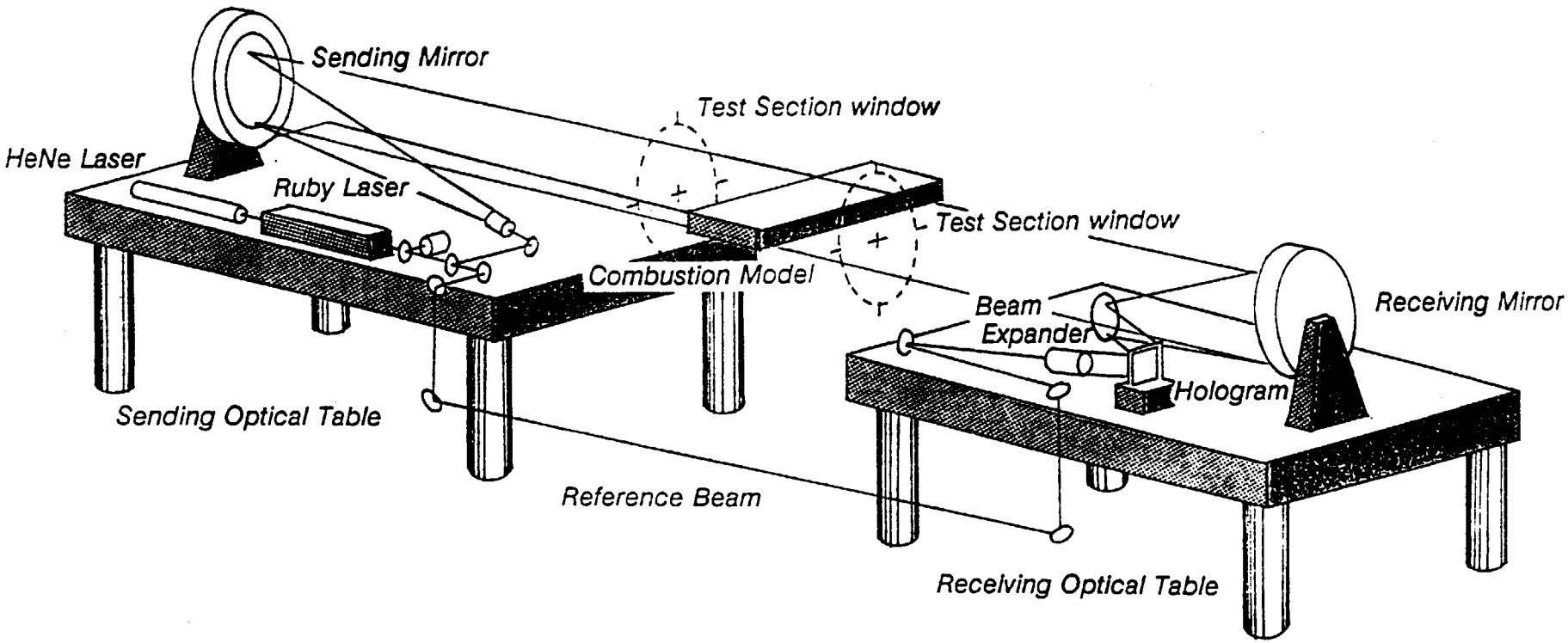


Figure 6. Schematic Diagram of LHI System

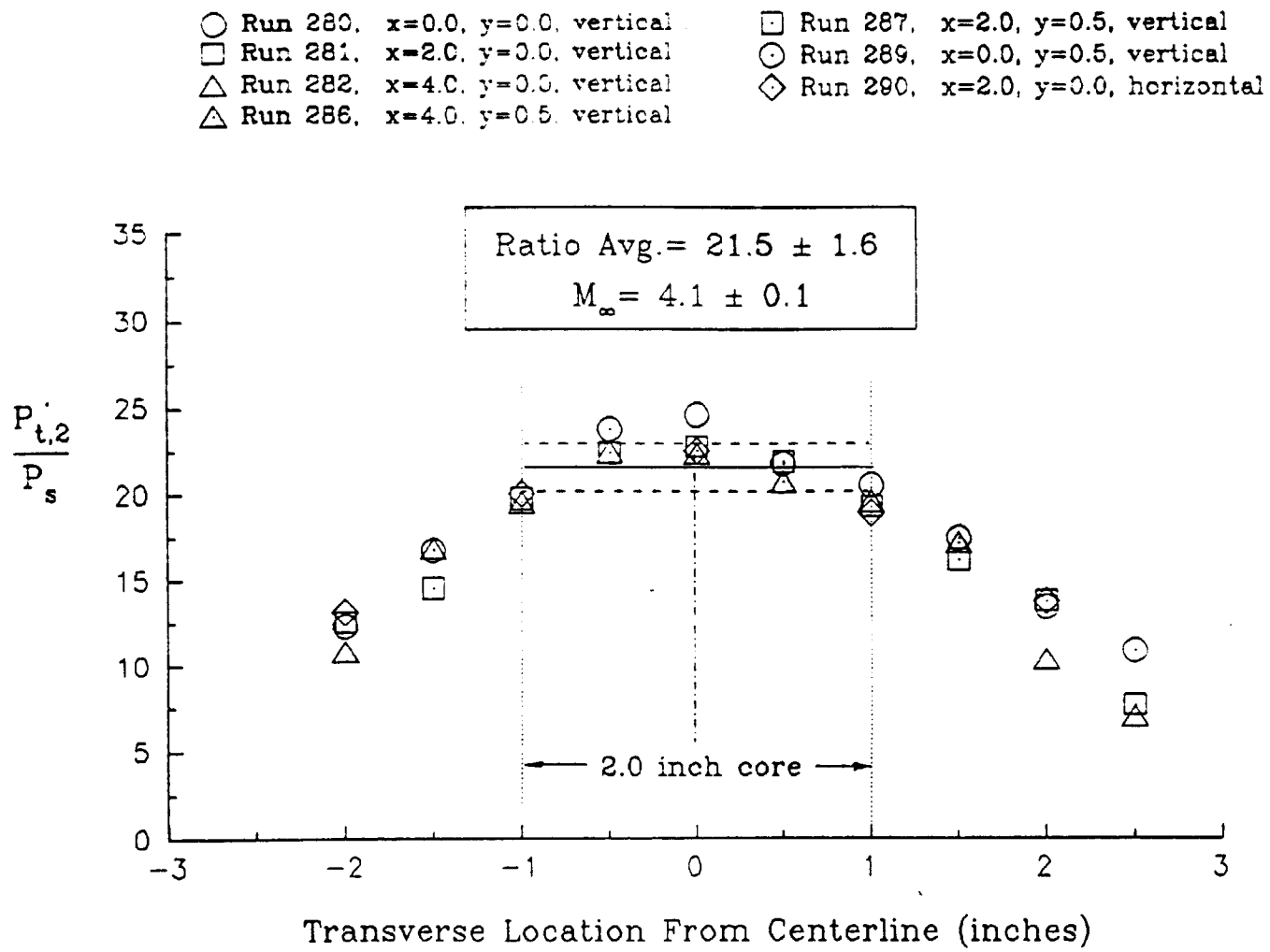


Figure 7. Test Section Pitot-to-Static Pressure Profile: M13.5 LP Condition

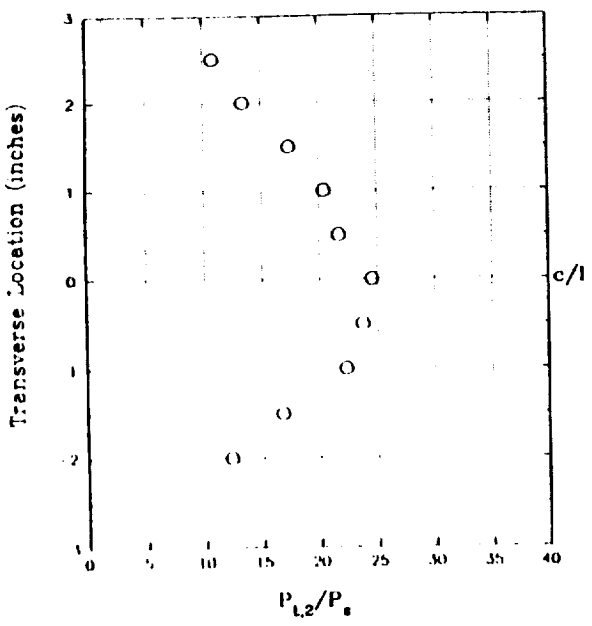


a) x=0.0 in.

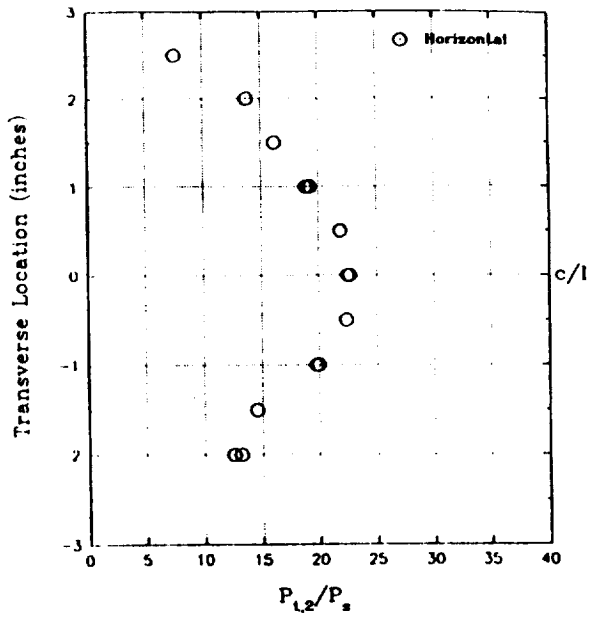


b) x=2.0 in.

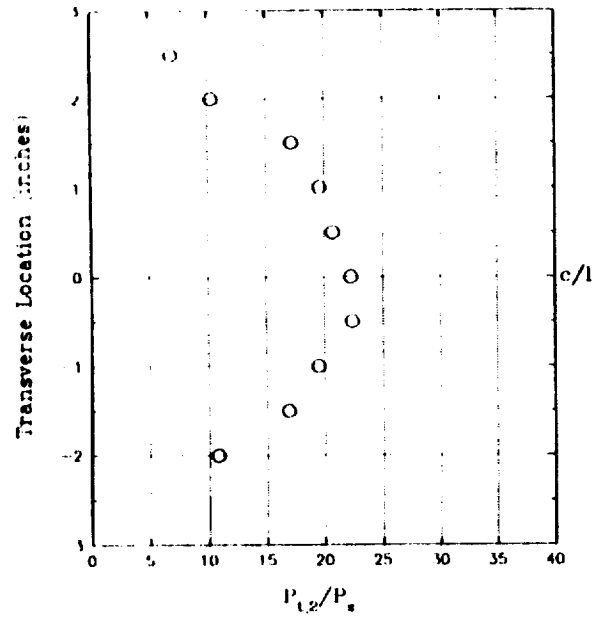


c) x=4.0 in.

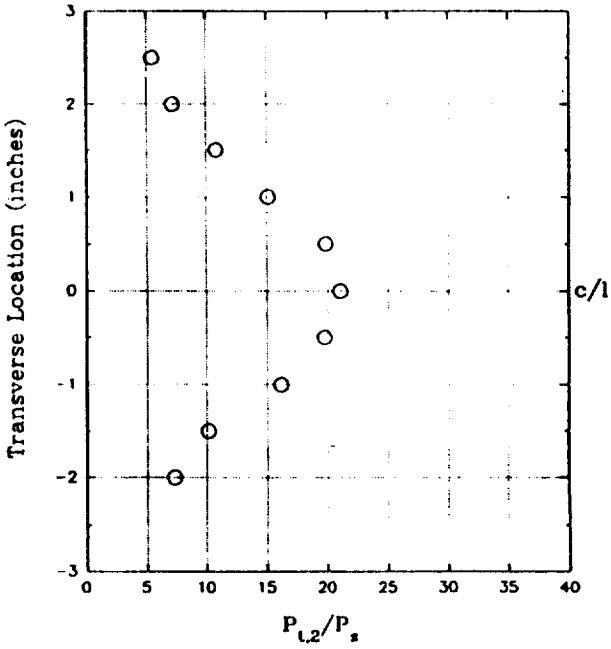


d) x=8.0 in.

Figure 8. Test Section $P_{t,2}/P_s$ at Various Axial Locations Downstream of Acceleration Chamber Exit Plane for M13.5 LP Condition

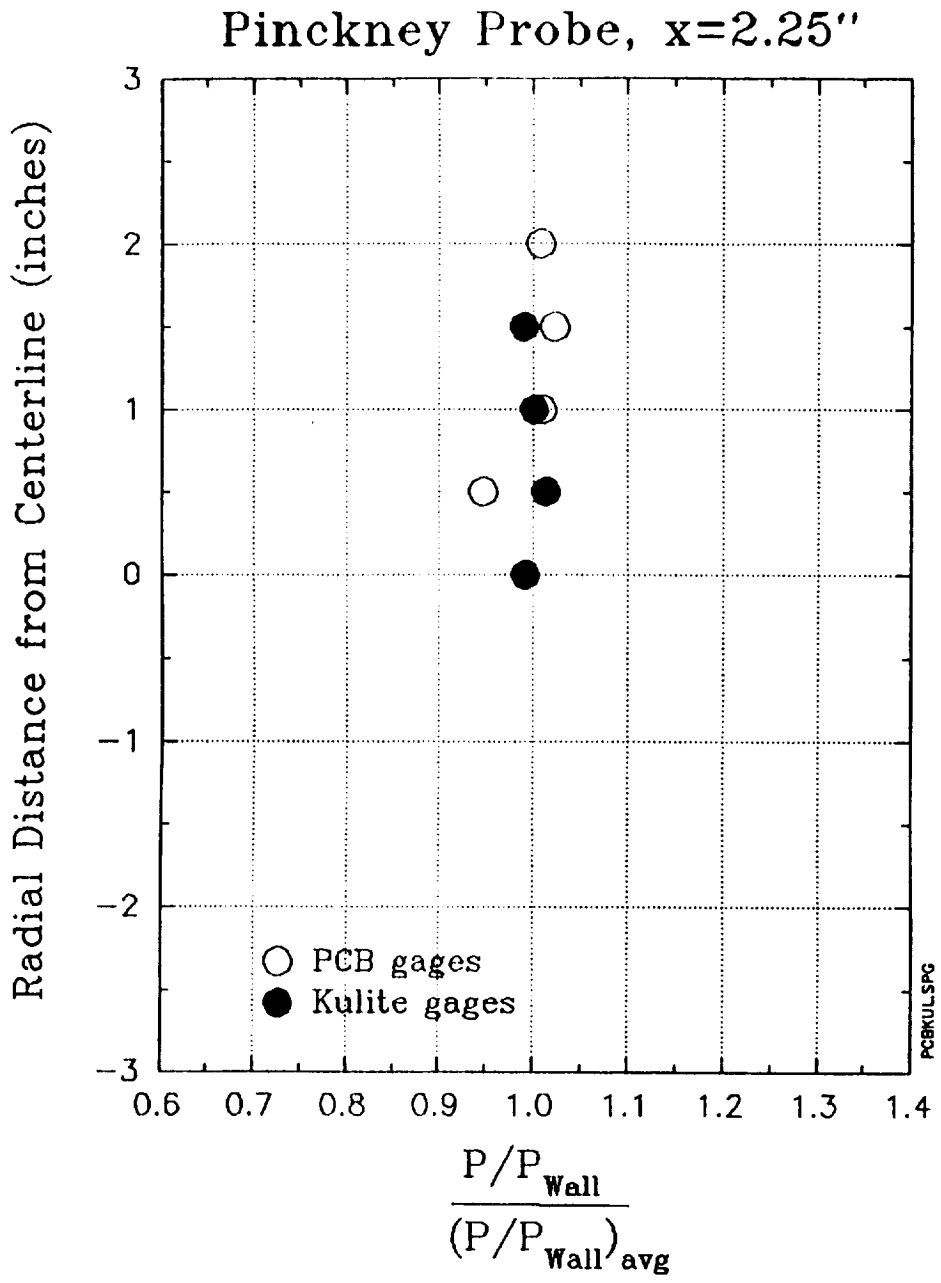


Figure 9. In-Stream Static Pressure Profile: M13.5 LP Condition

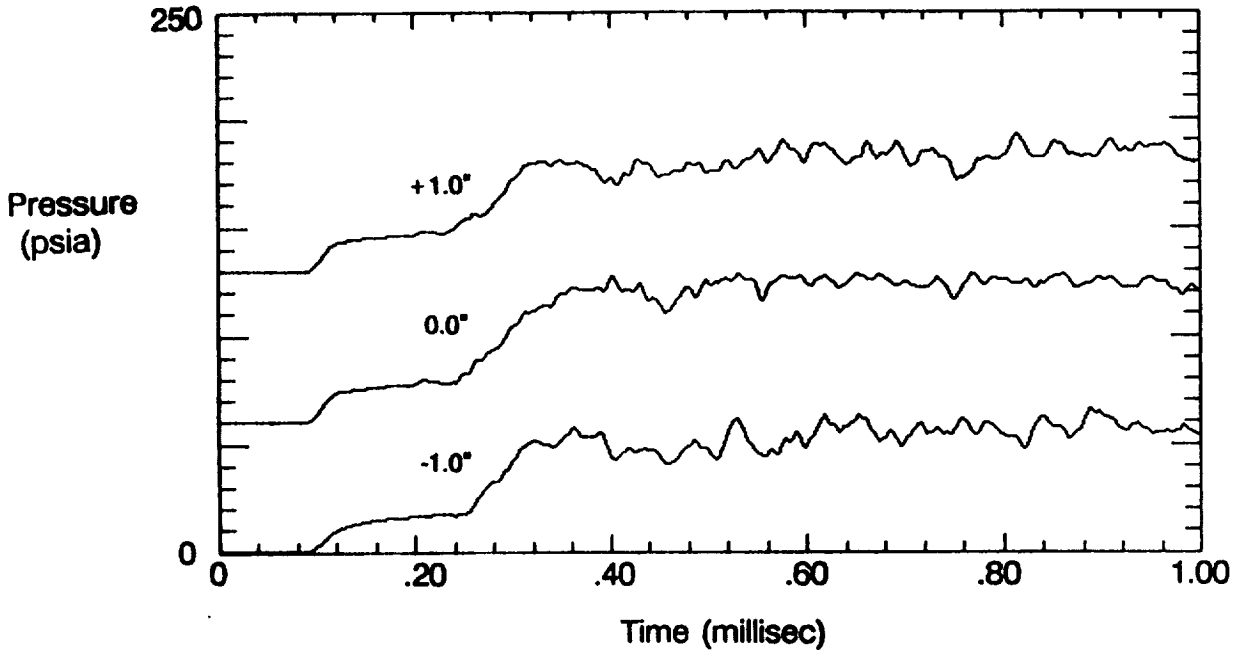


Figure 10. Typical Pitot Pressure Traces for M13.5 LP Condition

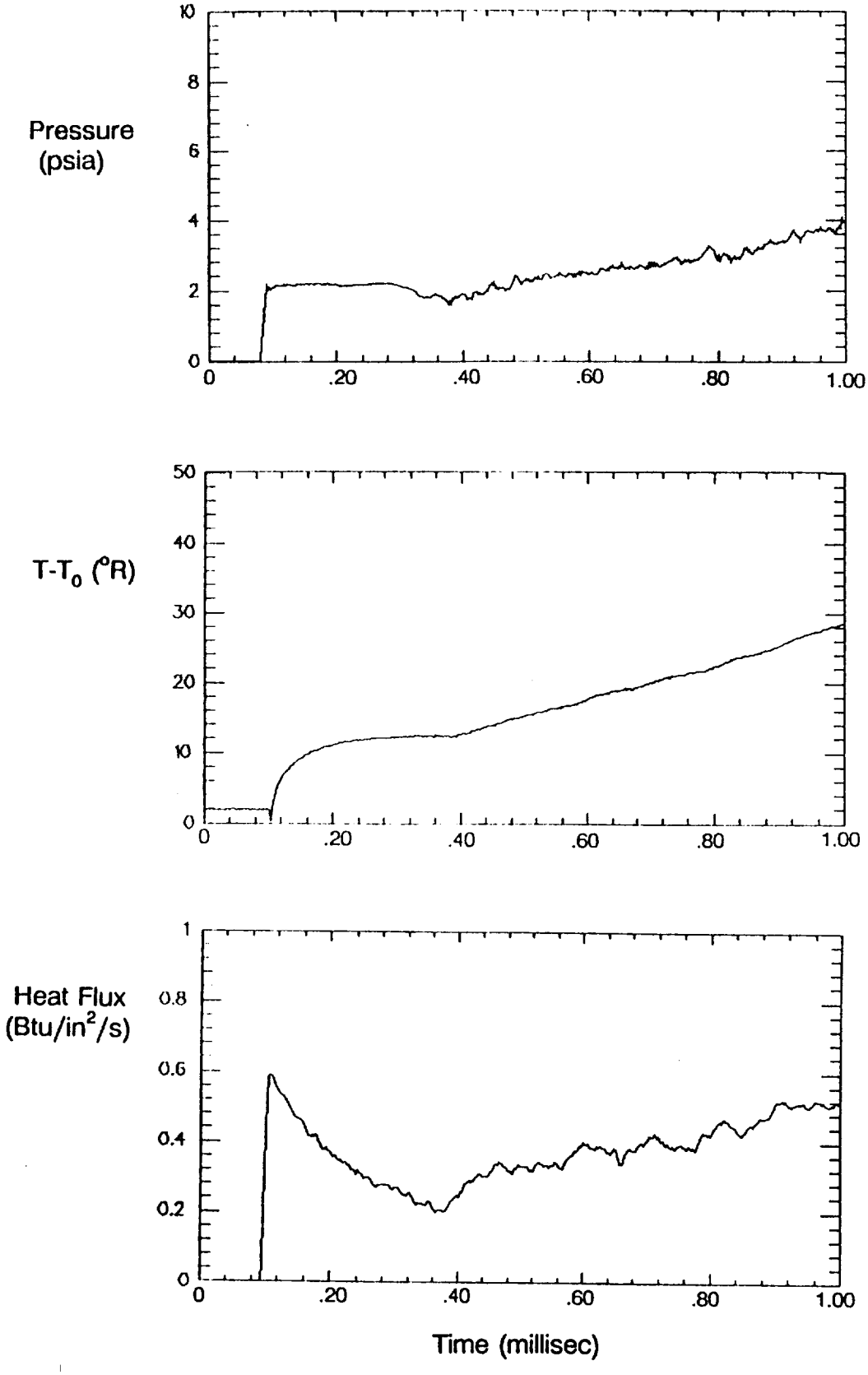


Figure 11. Wall Static Pressure, Temperature, and Heat Flux for M13.5 LP Condition

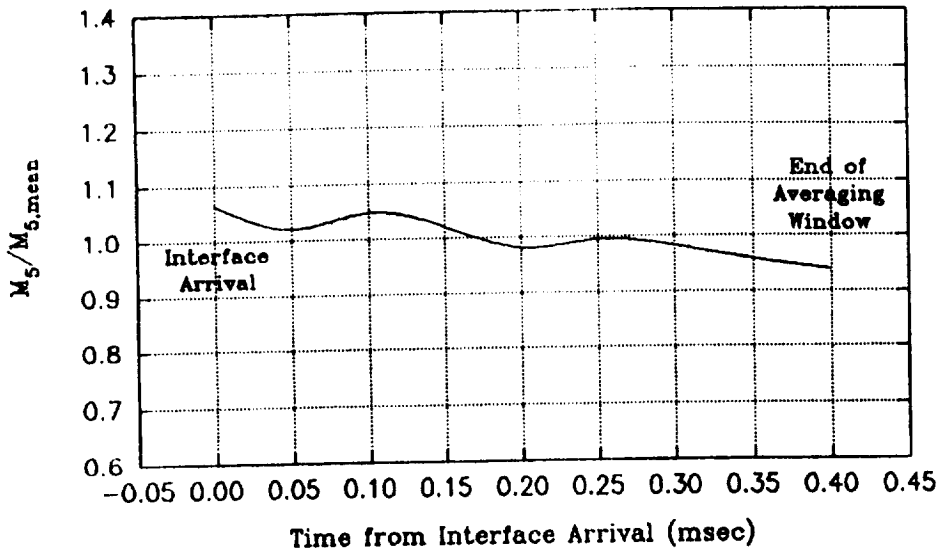


Figure 12. Test Section Mach Number vs. Time: M13.5 LP Condition

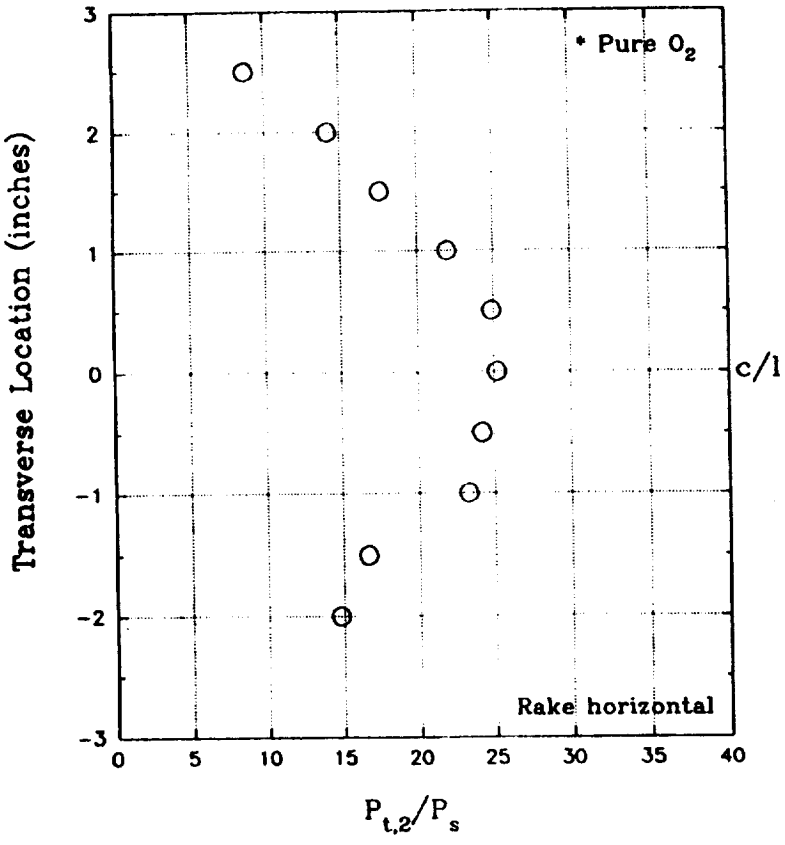


Figure 13. Test Section Pitot-to-Static Pressure Profile: M13.5 LP Condition for an $O_2$ Test Gas

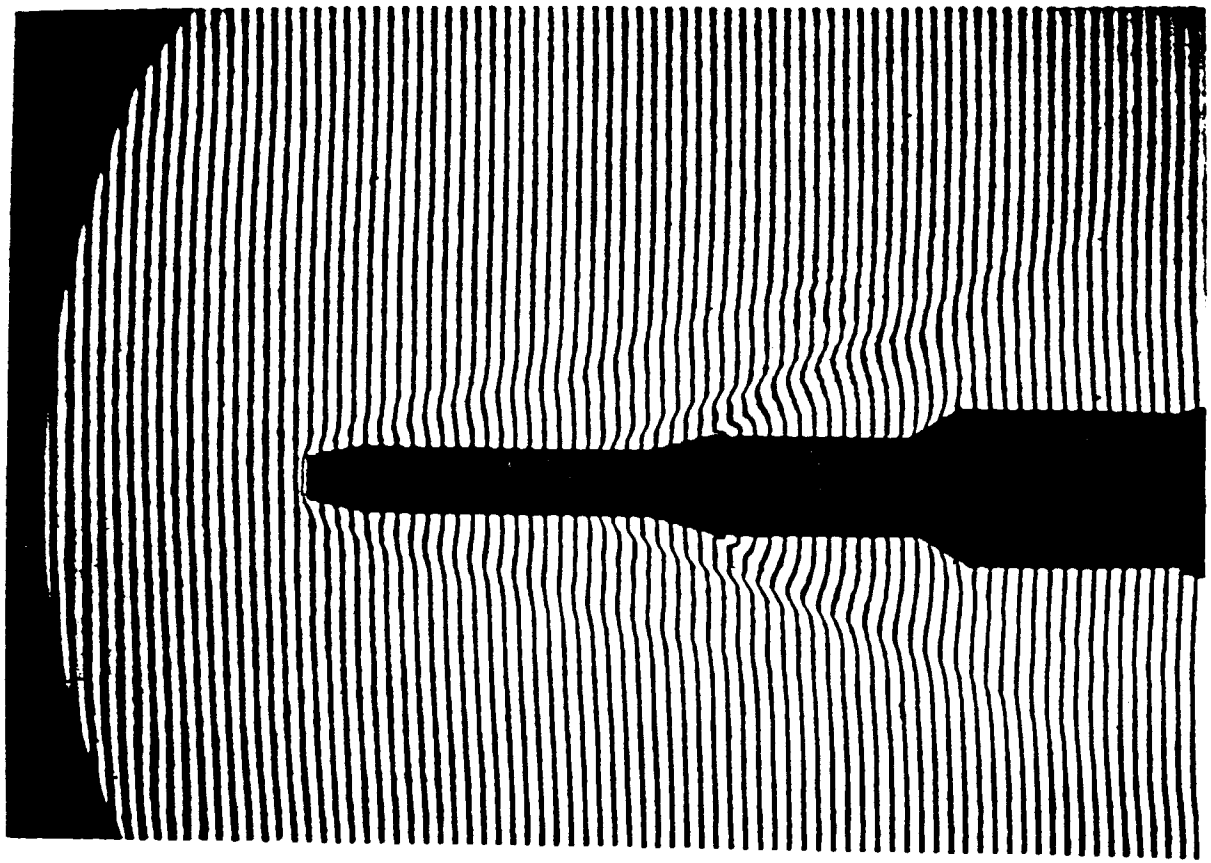

Figure 14. Finite Fringe Interferogram of Horizontal Pitot Rake: $O_2$ at M13.5 LP Condition

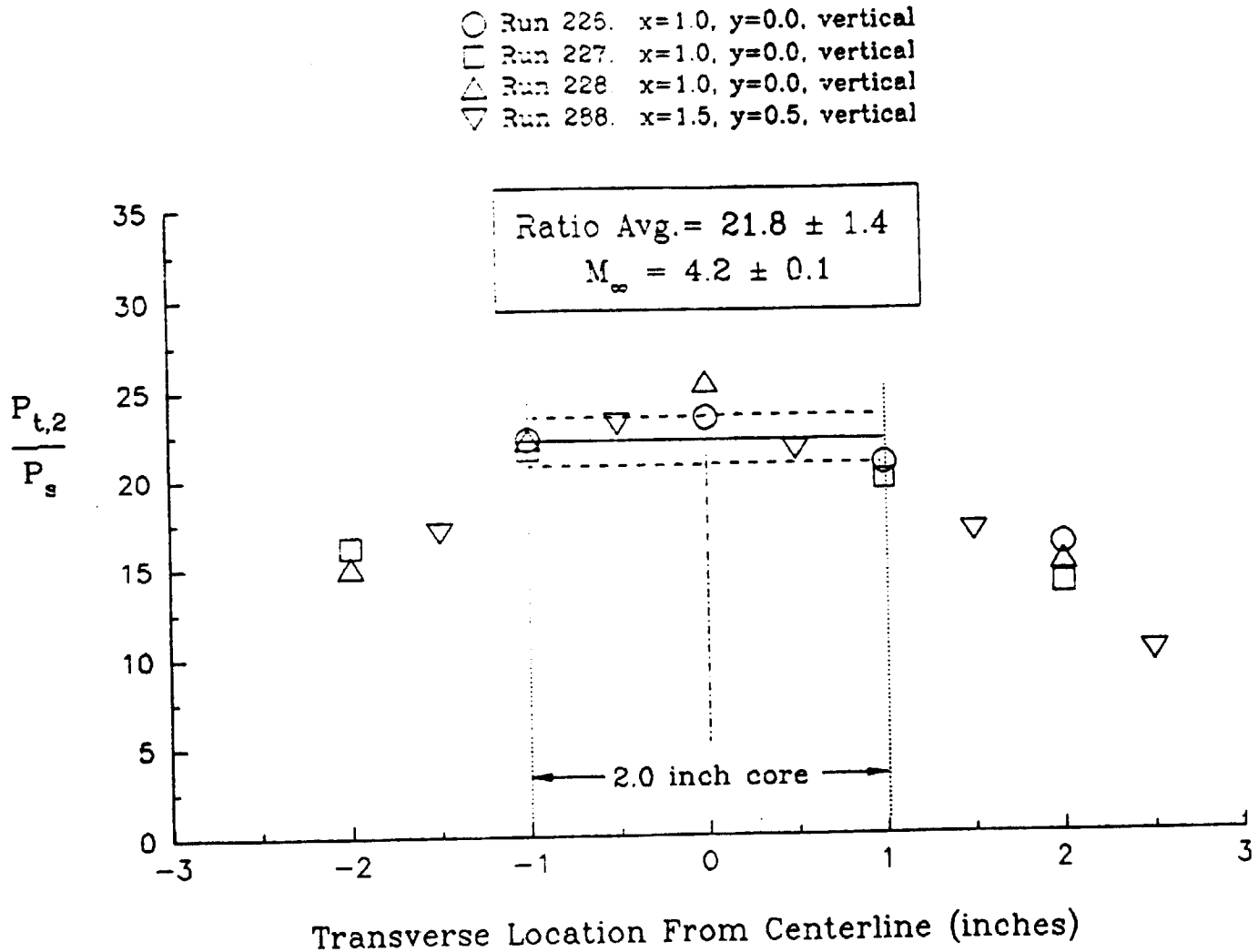


Figure 15. Test Section Pitot-to-Static Pressure Profile: M13.5 HP Condition

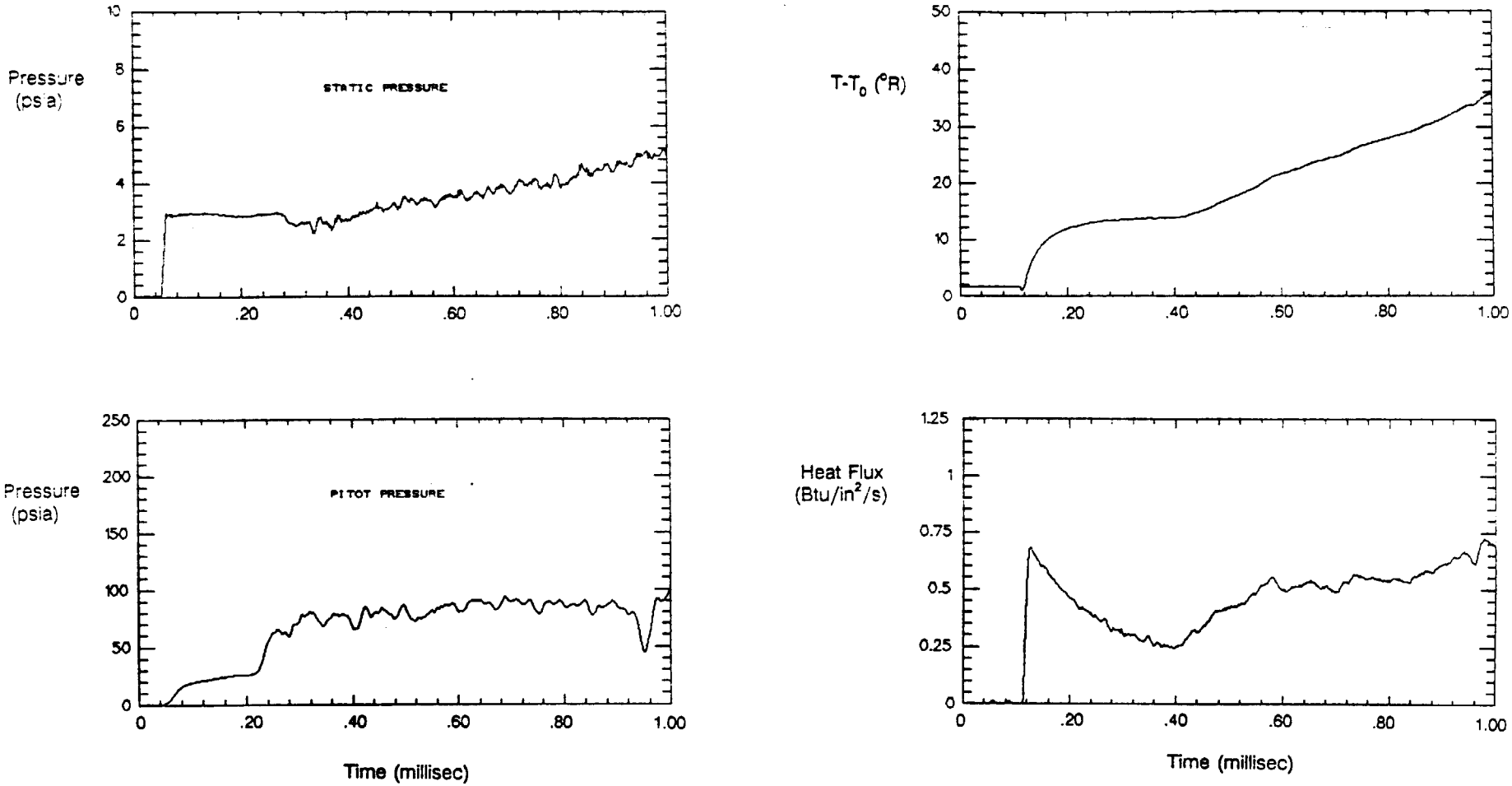


Figure 16. Pitot Pressure, Static Pressure, Wall Temperature and Heat Flux for M13.5 HP Condition

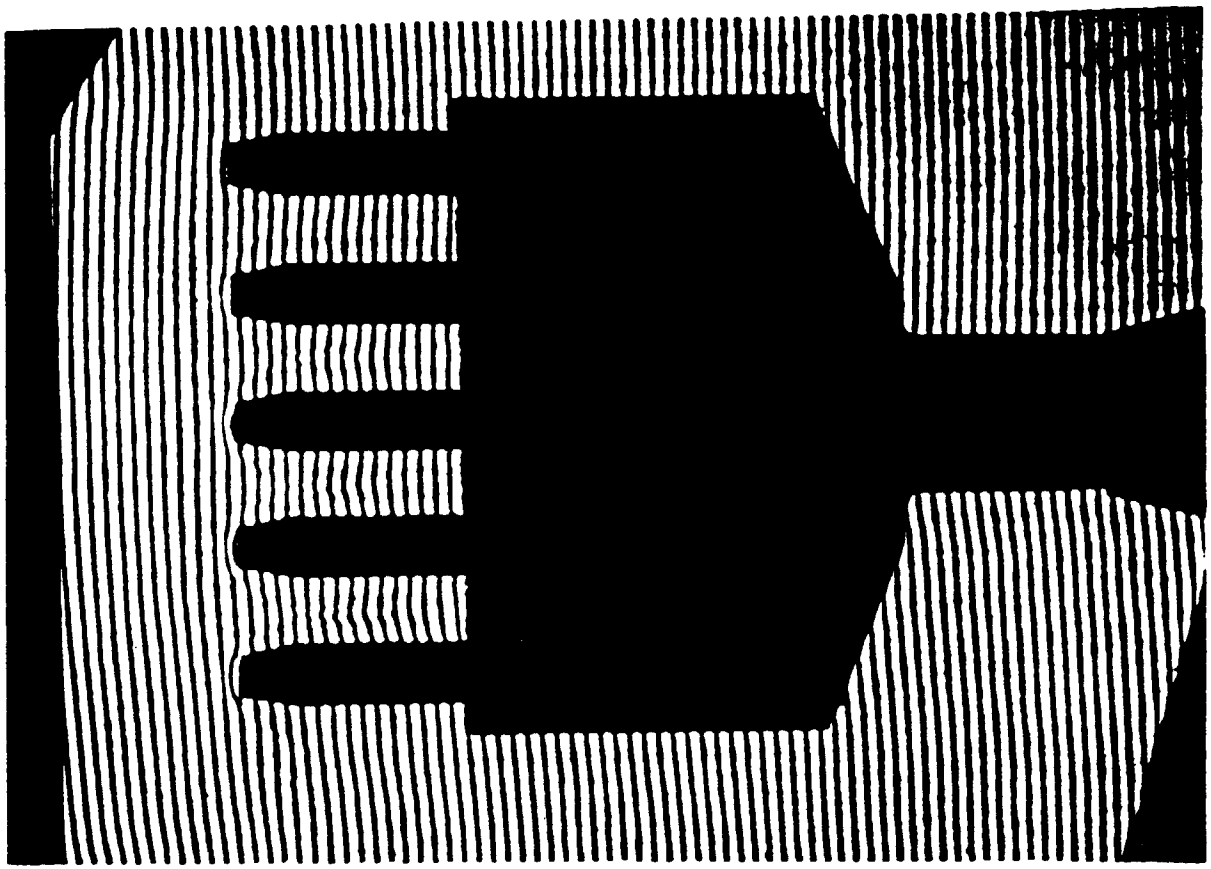

Figure 17. Finite Fringe Interferogram of Vertical Pitot Rake: M13.5 HP Condition

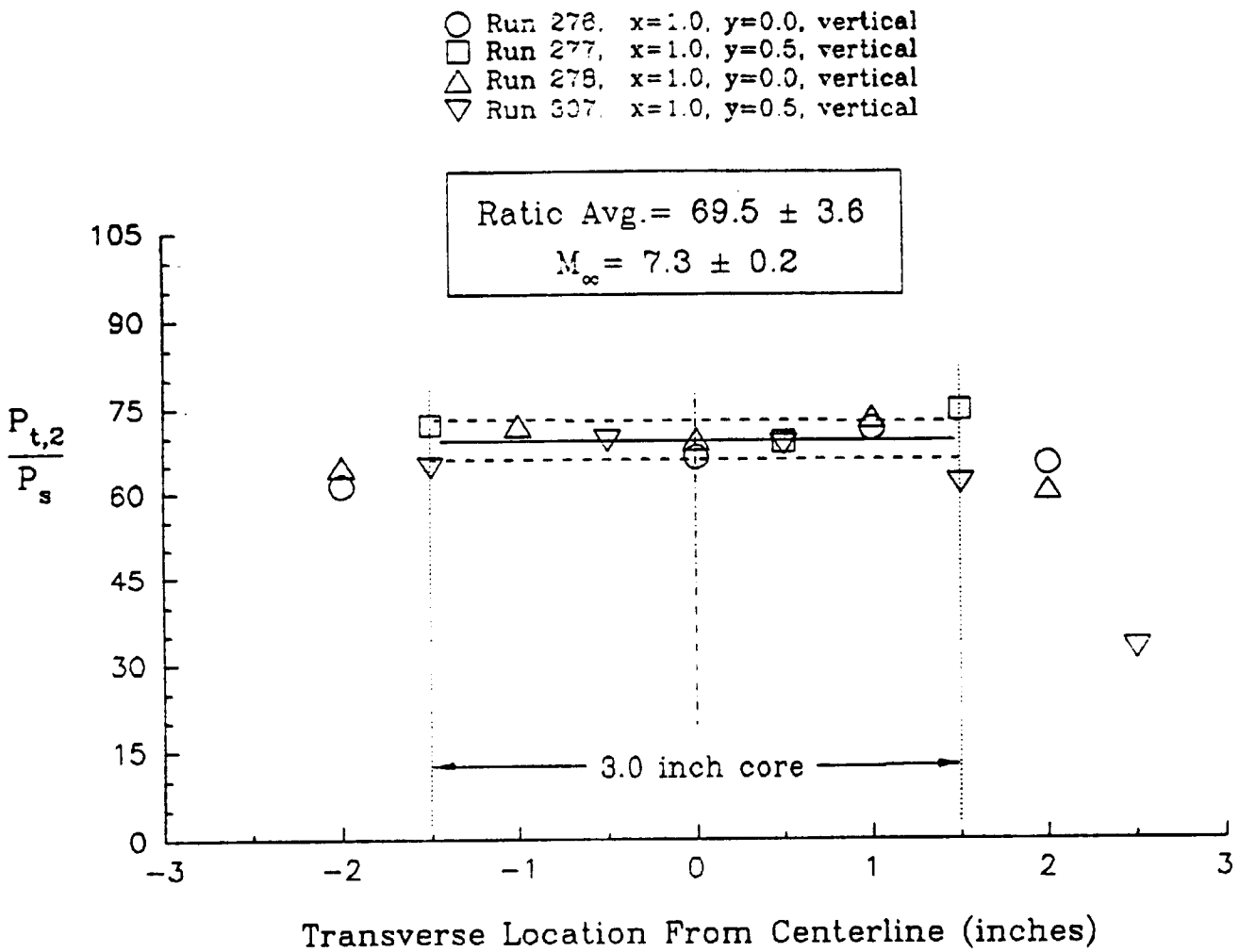


Figure 18. Test Section Pitot-to-Static Pressure Profile: M15 Condition

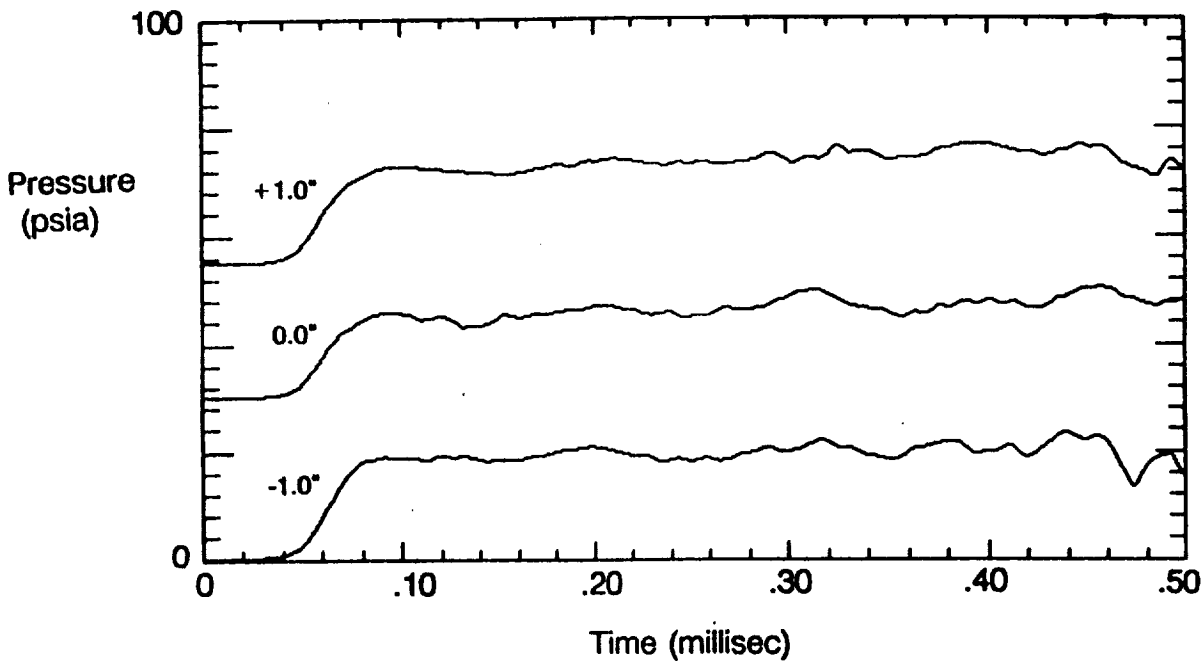


Figure 19. Typical Pitot Pressure Traces for M15 Condition

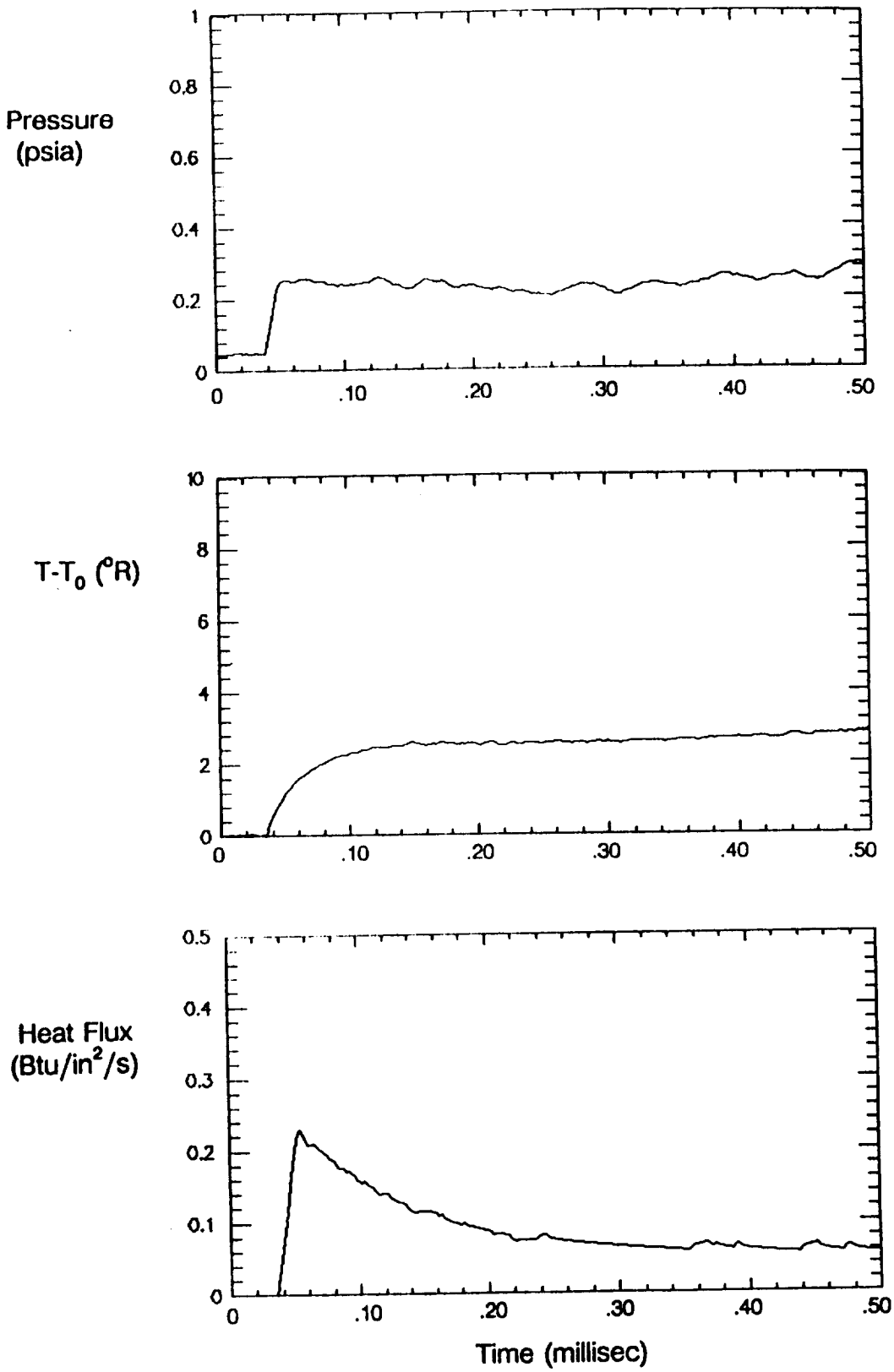


Figure 20. Wall Static Pressure, Temperature, and Heat Flux for M15 Condition

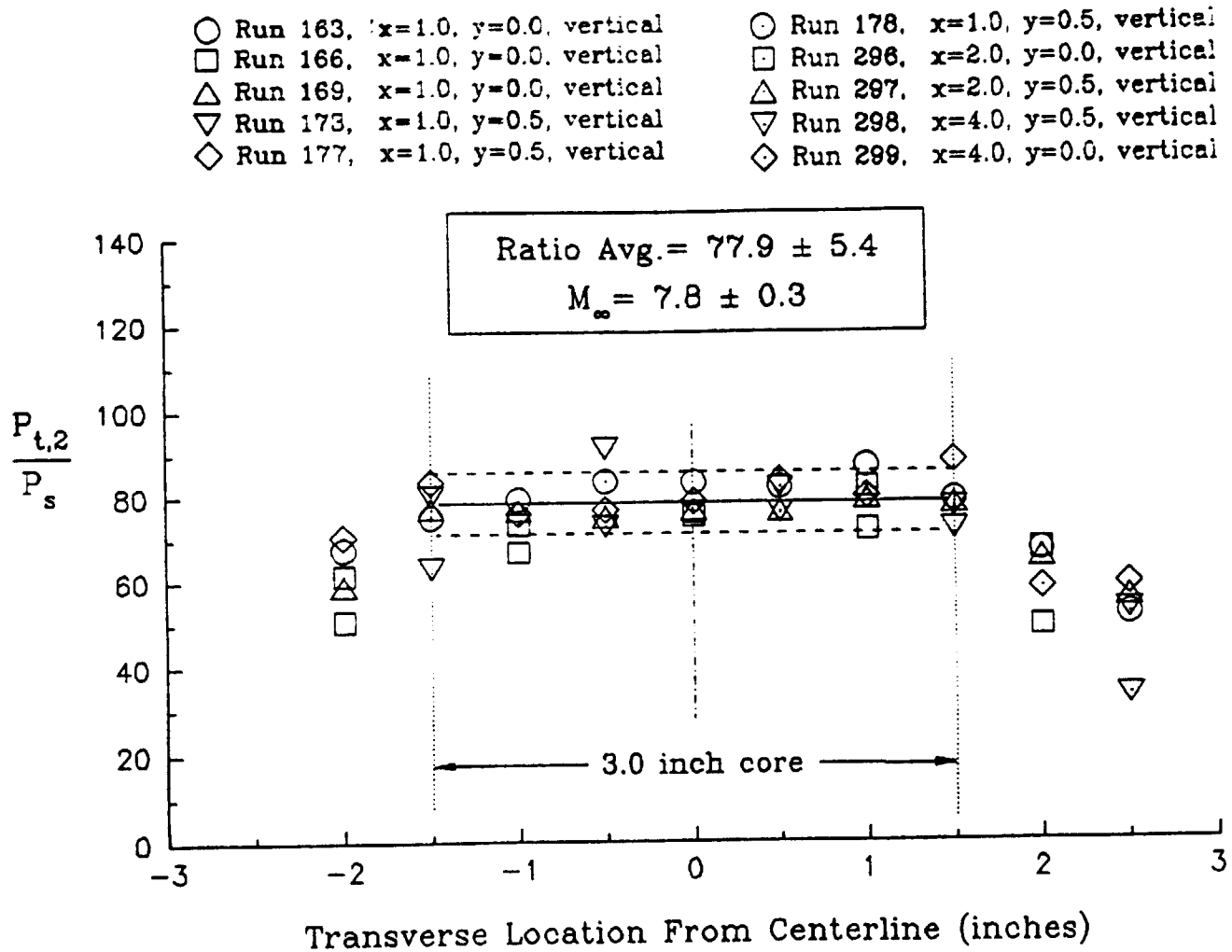


Figure 21. Test Section Pitot-to-Static Pressure Profile: M17 Condition

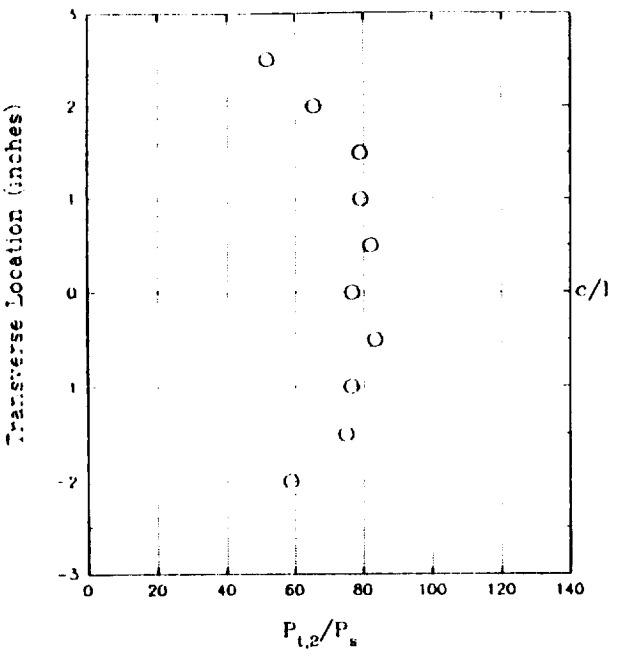


a) x=1.0 in.

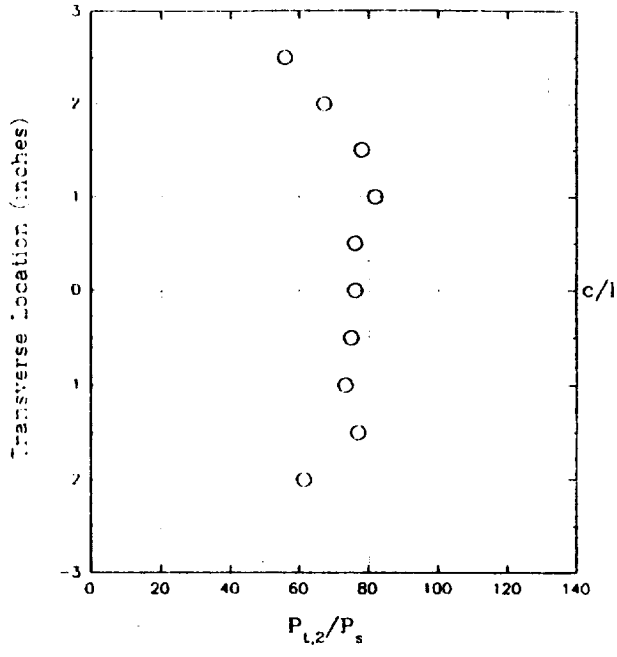


b) x=2.0 in.

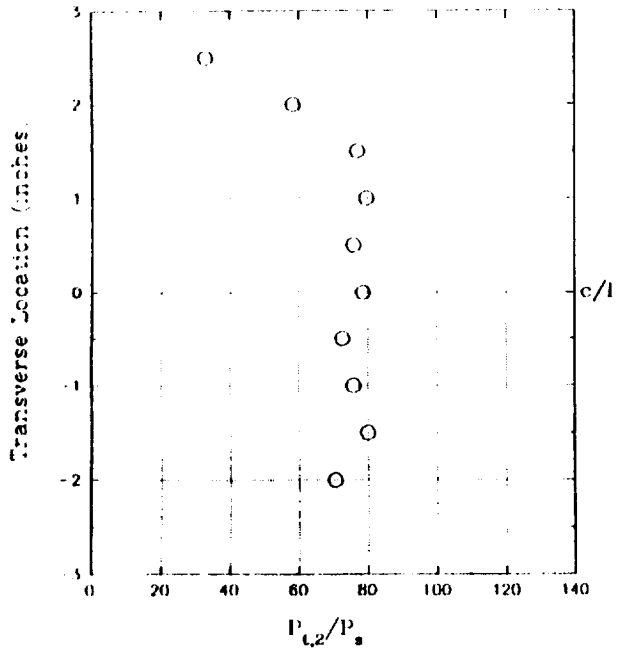


c) x=4.0 in.

Figure 22. Test Section $P_{t,2}/P_s$ at Various Axial Locations Downstream of Acceleration Chamber Exit Plane for M17 Condition

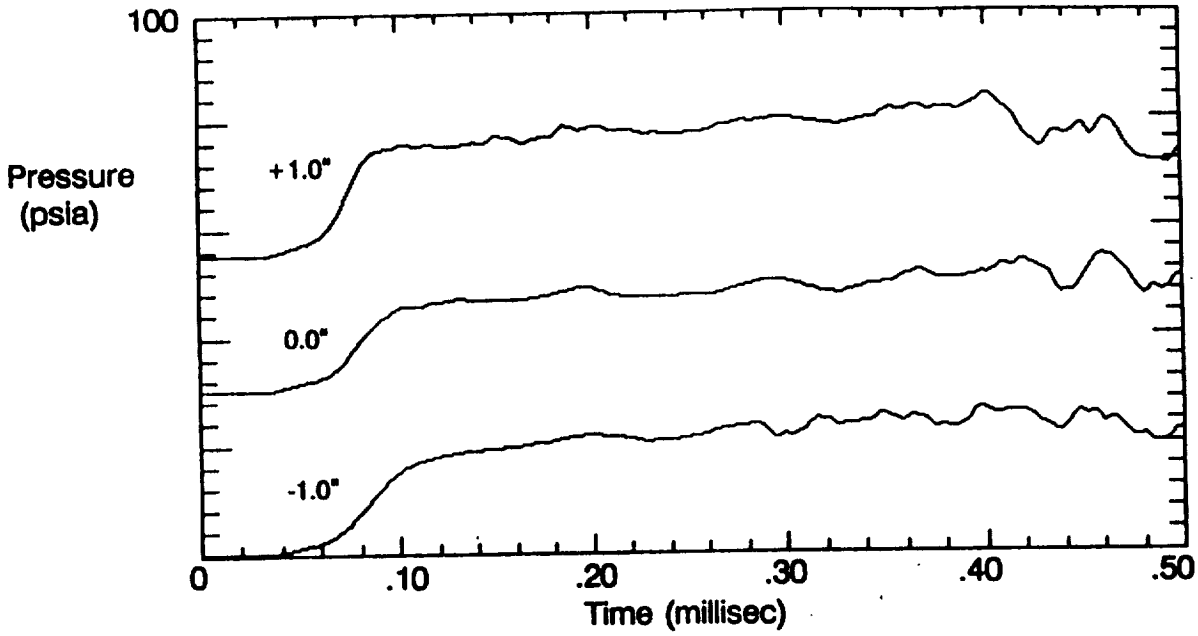


a) within core

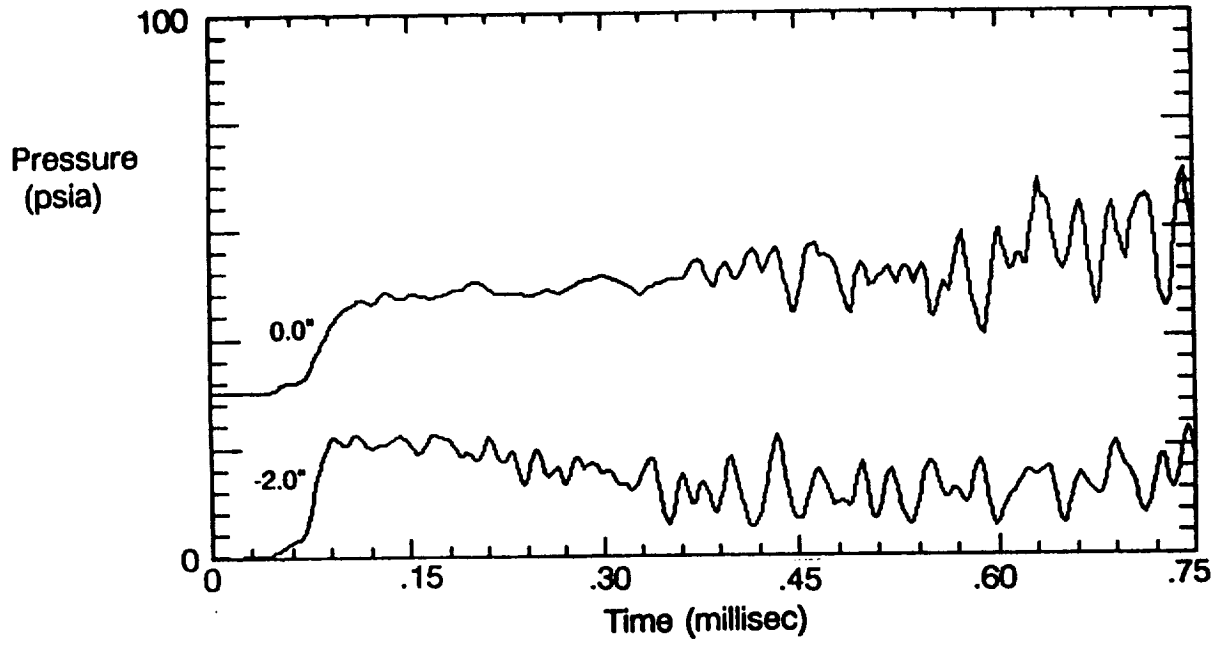


b) outside core and centerline comparison

Figure 23. Typical Pitot Pressure Traces for M17 Condition

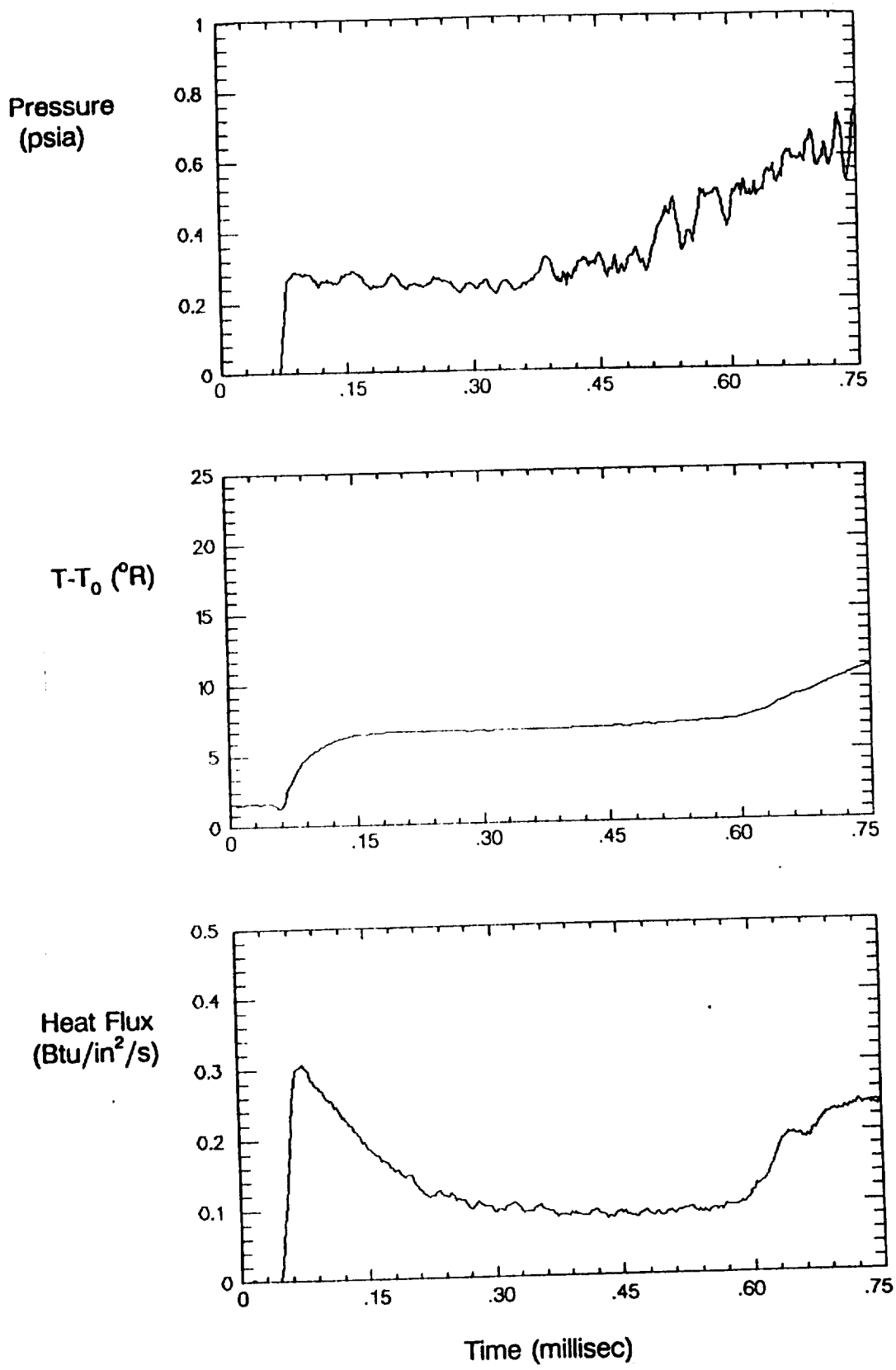


Figure 24. Wall Static Pressure, Temperature, and Heat Flux for M17 Condition

# REPORT DOCUMENTATION PAGE

*Form Approved*
*OMB No. 0704-0188*



| 1. AGENCY USE ONLY (*Leave blank*) | 2. REPORT DATE | 3. REPORT TYPE AND DATES COVERED |
|---|---|---|
| | December 1993 | Contractor Report, CY 1992 |

**4. TITLE AND SUBTITLE**
Calibration of HYPULSE for Hypervelocity Air Flows Corresponding to Flight Mach Numbers 13.5, 15, and 17

**5. FUNDING NUMBERS**
505-70-62-09
NAS1-18450
Task 27

**6. AUTHOR(S)**
John Calleja and Jose Tamagno

**7. PERFORMING ORGANIZATION NAME(S) AND ADDRESS(ES)**
General Applied Science Laboratories, Inc.
77 Raynor Avenue
Ronkonkoma, NY 11779

**8. PERFORMING ORGANIZATION REPORT NUMBER**
TR 335

**9. SPONSORING / MONITORING AGENCY NAME(S) AND ADDRESS(ES)**
National Aeronautics and Space Administration
Langley Research Center
Hampton, VA 23681-0001

**10. SPONSORING / MONITORING AGENCY REPORT NUMBER**
NASA CR-191578

**11. SUPPLEMENTARY NOTES**
Langley Technical Monitor: A. G. McLain

**12a. DISTRIBUTION / AVAILABILITY STATEMENT**
Unclassified - Unlimited

Subject Category 09

**12b. DISTRIBUTION CODE**

**13. ABSTRACT** (*Maximum 200 words*)

A series of air calibration tests were performed in GASL's HYPULSE facility in order to more accurately determine test section flow conditions for flows simulating total enthalpies in the Mach 13 to 17 range. Present calibration data supplements previous data and includes direct measurement of test section pitot and static pressure, acceleration tube wall pressure and heat transfer, and primary and secondary incident shock velocities. Useful test core diameters along with the corresponding free-stream conditions and usable testing times were determined. For the M13.5 condition, in-stream static pressure surveys showed the temporal and spacial uniformity of this quantity across the useful test core. In addition, finite fringe interferograms taken of the free-stream flow at the test section did not indicate the presence of any "strong" wave system for any of the conditions investigated.

| 14. SUBJECT TERMS | 15. NUMBER OF PAGES |
|---|---|
| Test facility, shock tube, shock wave | 60 |
| | 16. PRICE CODE: A04 |

| 17. SECURITY CLASSIFICATION OF REPORT | 18. SECURITY CLASSIFICATION OF THIS PAGE | 19. SECURITY CLASSIFICATION OF ABSTRACT | 20. LIMITATION OF ABSTRACT |
|---|---|---|---|
| Unclassified | Unclassified | Unclassified | |